1 **A dual-targeted purple acid phosphatase in *Arabidopsis thaliana***

2 **moderates carbon metabolism and its overexpression leads to faster**

3 **plant growth and higher seed yield**

4

5 Feng Sun[1], Pui Kit Suen[1], Youjun Zhang[1], Chao Liang[1], Chris Carrie[2], James Whelan[2],

6 Jane L. Ward[3], Nathaniel D. Hawkins[3], Liwen Jiang[4], Boon Leong Lim[1,*]

7 [1]School of Biological Sciences, the University of Hong Kong, Pokfulam, Hong Kong,

8 China.

9 [2] Australian Research Council Centre of Excellence in Plant Energy Biology,

10 University of Western Australia, Crawley WA 6009, Australia.

11 [3] National Centre for Plant and Microbial Metabolomics, Rothamsted Research, West

12 Common, Harpenden, Herts, AL5 2JQ, United Kingdom

13 [4]School of Life Sciences, Centre for Cell and Developmental Biology, the Chinese

14 University of Hong Kong.

15

16 Author for correspondence:

17 *Boon Leong Lim*

18 *Tel: +852 22990319*

19 *Email: bllim@hku.hk*

20 Word count for main body of the text: 6237

21 Word count for Introduction: 452

22 Word count for Materials and Methods: 2035

23 Word count for Results: 2384

24 Word count for Discussion: 1289

25 Word count for Acknowledgements: 77

26 The number of figures: 6

27 The number of tables: 2

28 The number of supporting figures: 11

29 The number of supporting tables: 3

30

31

32

1

1 **Summary**

2 • Overexpression of AtPAP2, a purple acid phosphatase (PAP) with a unique

3 C-terminal hydrophobic motif in Arabidopsis, resulted in earlier bolting and a

4 higher seed yield. Metabolite analysis showed that the shoots of AtPAP2

5 overexpression lines contained higher levels of sugars and tricarboxylic acid

6 metabolites. Enzyme assays showed that sucrose phosphate synthase (SPS) activity

7 was significantly upregulated in the overexpression lines. The higher SPS activity

8 arose from a higher level of SPS protein, and was independent of SnRK1.

9 • AtPAP2 was found to be targeted to both plastids and mitochondria via its

10 C-terminal hydrophobic motif. Ectopic expression of a truncated AtPAP2 without

11 this C-terminal motif in Arabidopsis indicated that the subcellular localization of

12 AtPAP2 is essential for its biological actions.

13 • Plant PAPs are generally considered to mediate phosphorus acquisition and

14 redistribution. AtPAP2 is the first PAP shown to modulate carbon metabolism and

15 the first shown to be dual-targeted to both plastids and mitochondria by a

16 C-terminal targeting signal.

17 • One PAP-like sequence carrying a hydrophobic C-terminal motif could be

18 identified in the genome of the smallest free-living photosynthetic eukaryote,

19 *Ostreococcus tauri*. This might reflect a common ancestral function of AtPAP2-like

20 sequences in the regulation of carbon metabolism.

21

22 **Key words:** purple acid phosphatase, sugars, flowering, sucrose phosphate synthase,

23 TCA, chloroplasts, mitochondria

24

25

2

1 **Introduction**

2   Modification of carbon metabolism is a prime target for maximizing crop

3 productivity (Sharma-Natu & Ghildiyal, 2005). Sugars not only represent an energy

4 product from photosynthesis, but also play roles in complex cellular signaling pathways

5 (Rolland *et al.*, 2002; Gibson, 2005; Rolland *et al.*, 2006), which are mediated by a

6 variety of protein kinases (PKs), and protein phosphatases (PPs) (Baena-Gonzalez &

7 Sheen, 2008; Smeekens *et al.*, 2010; Zheng *et al.*, 2010). In *Arabidopsis thaliana*,

8 SNF1-related kinase (SnRK1) is a central resource regulator in response to energy

9 deficiency (Baena-Gonzalez *et al.*, 2007; Baena-Gonzalez & Sheen, 2008). By

10 phosphorylating and inactivating sucrose phosphate synthase (SPS), nitrate reductase

11 (NR), and a few other metabolic enzymes (Lunn & MacRae, 2003; Polge *et al.*, 2008),

12 energy and resources were reallocated from anabolic pathways (e.g. sucrose synthesis

13 and nitrogen assimilation) to catabolic pathways (Smeekens *et al.*, 2010). In

14 Arabidopsis, geminivirus Rep interacting kinases (GRIK1 and GRIK2) activate SnRK1

15 by phosphorylating it at the T_{175} residue (Shen & Hanley-Bowdoin, 2006; Shen *et al.*,

16 2009).

17   PPs regulate a variety of genes involved in sugar metabolism, such as those encoding

18 the two major amylases of the tuberous root of sweet potato (Takeda *et al.*, 1994), the

19 ADP-glucose pyrophosphorylase subunit in sweet potato and Arabidopsis (Takeda *et*

20 *al.*, 1994; Siedlecka *et al.*, 2003), and the enzymes for fructan synthesis (Martinez-Noel

21 *et al.*, 2009), the UDP-glucose pyrophosphorylase, and the sucrose synthase of

22 Arabidopsis (Winter *et al.*, 1997; Ciereszko *et al.*, 2001; Martinez-Noel *et al.*, 2009).

23 Okadaic acid, a PP inhibitor, prevents activation of SPS and impairs sucrose

24 accumulation in leaves (Huber *et al.*, 1992). Okadaic acid also induces vacuolar acid

25 invertase transcription, suggesting that PP activity plays a role in carbon partitioning

3

1   (Martinez-Noel *et al.*, 2009).

2   Purple acid phosphatases (PAPs) represent a large group of nonspecific acid

3   phosphatases (Schenk *et al.*, 2000). In the Arabidopsis genome, 29 PAP genes have

4   been identified based on sequence comparison (Zhu *et al.*, 2005). Plant PAPs are

5   considered to mediate phosphorus acquisition and redistribution based on their ability

6   to hydrolyze phosphorus compounds (Cashikar *et al.*, 1997; Lung *et al.*, 2008; Kuang *et*

7   *al.*, 2009). Certain PAPs also exhibit peroxidase activity, such as GmPAP3 (Liao *et al.*,

8   2003; Li *et al.*, 2008) and AtPAP17 (del Pozo *et al.*, 1999). Recent studies also showed

9   that a tobacco PAP (NtPAP12) can modulate polysaccharide synthesis; it can upregulate

10   β-glucan synthesis and cellulose deposition in the cell wall by dephosphorylating

11   α-xylosidase and β-glucosidase (Kaida *et al.*, 2009; Kaida *et al.*, 2010).

12   In this study, we show that AtPAP2 is dual-targeted to mitochondria and plastids via

13   a novel and unique C-terminal transmembrane targeting signal. Overexpression of

14   AtPAP2 significantly enhanced the growth rate and seed yield of Arabidopsis, through

15   increased sucrose phosphate synthase activity.

16

4

1   **Materials and methods**

2   Plant materials and growth conditions

3   WT *Arabidopsis thaliana* ecotype Columbia (Col-0) was used in this study. The

4   T-DNA mutant of AT1G13900 (Salk_013567, ecotype Col-0) and AT2G03450

5   (Salk_129905, ecotype Col-0) were obtained from the Arabidopsis Biological

6   Resource Center (http://abrc.osu.edu). Chilled Arabidopsis seeds were

7   surface-sterilized with 20% (v/v) bleach for 15 minutes, washed, and plated on

8   Murashige and Skoog (MS) medium supplemented with 2% (w/v) sucrose for 10 days.

9   Seedlings with the same size were transferred to soil under a 16-hr light (22°C)/8-hr

10   dark (18°C) regime (long day, LD) or an 8-hr light (22°C)/16-hr dark (18°C) regime

11   (short day, SD) under a light intensity of 120–150 µmol m^{-2} s^{-1}. The pots were placed in

12   the growth chamber in a randomized design. Bolting time was measured when the

13   primary inflorescence reached 1 cm above the rosette leaves. This observation of

14   phenotype was repeated at least three times (n = 10–15).

15   Sequence alignment and phylogenetic analysis

16   Sequence data was retrieved from the TAIR website (http://www.arabidopsis.org) and

17   the National Center for Biotechnology Information (NCBI)

18   (http://www.ncbi.nlm.nih.gov). Homology searches in GenBank were done using the

19   Basic Local Alignment Search Tool server (http://www.ncbi.nlm.nih.gov/BLAST/).

20   Multiple alignments of protein sequences were performed by MEGA 4.1 (Beta 3)

21   software (Kumar *et al.*, 2004) (http://www.megasoftware.net) using the Clustal X and

22   N-J plot programs (Saitou & Nei, 1987). The amino acid sequences were aligned by

23   CLC sequence viewer 6.3 software (http://www.clcbio.com). Protein expression

5

1   patterns were analyzed via the spot history microarray analysis tool

2   (http://www.affymetrix.Arabidopsis.info/narrays/experimentbrowse.pl). Signal peptide

3   and transmembrane motif were predicted by the SignalP and TMHMM programs

4   (http://www.cbs.dtu.dk/services).

5   Generation of specific anti-AtPAP2 antiserum

6   A fragment of *AtPAP2* cDNA corresponding to the N-terminus of AtPAP2 (a.a.

7   25-144) was amplified by primers P2AbF and P2AbR. This region was selected to

8   avoid cross-reactivity toward other AtPAPs. The PCR product was digested with *Sac*I

9   and *Kpn*I and fused with the N-terminal His-tag of vector pRSET-A (Invitrogen, H.K.)

10   and the resulting plasmids were transformed into *Escherichia coli* strain BL21 (DE3).

11   The overexpressed fusion protein in the inclusion bodies was solubilized in extraction

12   buffer A (20 mM Tris-HCl, pH 7.5, 150 mM NaCl, 8 M urea) and purified by a HisTrap

13   FF column (GE Healthcare) using buffer A containing 100 mM imidazole. The eluted

14   protein was dialyzed in 20 mM PBS, pH 7.2 to remove urea. The antigen was further

15   gel-purified before being used for rabbit immunization. The specificity of this

16   antiserum was confirmed by western blotting analysis on the proteins isolated from

17   wild type (WT) and the T-DNA insertion line (Fig. S3d).

18   Expression of AtPAP2 under P-starvation and sugar treatments

19   Arabidopsis plants were grown in phosphate (Pi) starvation MS medium (0 mM Pi)

20   for 5 days and then transferred to complete MS medium for 0, 2, 4, 6 or 8 days.

21   Alternatively, plants were grown on MS agar for 7 days before transfer to Pi starvation

22   medium for 0, 2, 4, 7 or 10 days (del Pozo *et al.*, 1999). For sugar treatments, 5-day-old

23   seedlings on MS agar plates were transferred to solid MS medium containing a sucrose,

1   glucose, sorbitol or mannitol gradient (% w/v) for 24 hr. Total protein isolated from

2   seedlings was analyzed by western blot analysis using AtPAP2 antiserum.

Generation of AtPAP2 overexpression lines in Arabidopsis

4   The full-length coding region of the *AtPAP2* cDNA (AT1G13900) was amplified by

5   Pfx DNA polymerase (Invitrogen) using primers P2YF and P2NR. The resulting

6   product (1,971 bp) was initially cloned into vector pGEM-T Easy (Promega, H. K.) and

7   then subcloned into the binary vector pBA002 downstream of the cauliflower mosaic

8   virus (CaMV) 35S promoter (pBA002-CaMV35: *AtPAP2*). The vector was then

9   introduced into *Agrobacterium tumefaciens* strain GV3101 and then transformed by the

10   floral dip method (Clough & Bent, 1998) into WT plants. Homozygous CaMV35S:

11   *AtPAP2* OE lines were selected on MS plates containing 5 mg/L glufosinate ammonium

12   (Riedel-deHaen, Germany). Resistant lines were transferred to soil to grow to maturity,

13   and their transgenic status was confirmed by genomic PCR and western blot analyses.

14   Homozygous T3 seeds of the OE plants were used for further analysis. A construct of a

15   truncated *AtPAP2* fragment without its C-terminus (P2NC) was generated by PCR

16   using primers P2YF and P2NCR and cloned in the pBA002 vector. *AtPAP2* with a

17   deleted signal peptide (P2NS) was amplified with primers P2NSF and P2NR and

18   cloned into the pCXSN vector (Chen *et al.*, 2009). All primers used are listed in Table

19   S3.

Characterization of homozygous *AtPAP2* T-DNA line

21   A T-DNA insertion line of *AtPAP2* gene (Salk_013567) in the Col ecotype was

22   obtained from TAIR. The homozygous T-DNA line was verified by genomic PCR

23   screening using the T-DNA left border primer LBa1 and *AtPAP2* gene-specific primer

7

1   LP2 and reverse primer RP2 (SIGnAL database). The T-DNA insertion site was

2   confirmed by DNA sequencing of the PCR product.

Subcellular localization of AtPAP2

4   The putative signal peptide (SP) and the transmembrane domain and cytoplasmic tail

5   (TMD/CT) were PCR-amplified from full-length *AtPAP2* cDNA and cloned into a GFP

6   vector in pBI221 to generate SP-GFP, GFP-TMD/CT and SP-GFP-TMD/CT using

7   full-length *AtPAP2* cDNA as template and the primer sets listed in Table S3. Organelle

8   markers were used to elucidate the subcellular localization of *AtPAP2*-GFP constructs.

9   Transient expression in WT Arabidopsis PSB-D cell culture was performed as

10   described previously (Miao & Jiang, 2007). Generally, PSB-D cells at day 5 after

11   subculture were collected for protoplast preparation. Plasmids were electroporated into

12   protoplasts and incubated at 26°C for 13 hr before being observed under a confocal

13   laser scanning microscope. Protoplasts were incubated for 5 min at room temperature

14   with MitoTracker Orange (CMTMRos, Molecular Probes) before analysis. Confocal

15   images were collected with a Fluoview FV1000 microscope (Olympus, Japan) with a

16   60x objective water lens. The settings for collecting confocal images within the linear

17   range were described previously (Jiang & Rogers, 1998; Tse *et al.*, 2004). Images were

18   processed using Adobe Photoshop software (Jiang & Rogers, 1998).

Organelle isolation and western blot analysis

20   Mitochondria and chloroplasts were isolated from 10-day-old Arabidopsis seedlings

21   as previously described (Lister *et al.*, 2007; Kubis *et al.*, 2008). Proteins (25 μg) were

22   resolved by SDS-PAGE and transferred to Hybond-C nitrocellulose membranes, then

23   immunodetected as previously described (Carrie *et al.*, 2008). The antibodies used,

1   Tom40 (Carrie *et al.*, 2009a; Carrie *et al.*, 2009b) and Risp (Carrie *et al.*, 2010), have

2   been described previously. Antibodies to CoxII, Rubisco large subunit and Rubisco

3   small subunit (SSU) were purchased from Agrisera (Sweden).

4   Measurement of soluble sugars and starch in Arabidopsis

5   Soluble sugars were extracted from Arabidopsis using the chloroform/methanol

6   method (Antonio *et al.*, 2007). Liquid chromatography-MS/MS spectrophotometry was

7   employed for sugar measurement. Filtered samples (10 µl) were injected into an HP

8   1100 HPLC system (Agilent Technologies, Palo Alto, CA, USA) connected to a

9   zwitterionic ZIC-HILIC column (3.5 µm, 150 mm x 2.1 mm i.d.; SeQuant, Umea,

10 Sweden) (Antonio *et al.*, 2008). Separation was performed using a solvent system of

11 0.1% (v/v) formic acid in water (A) and 0.1% (v/v) formic acid in methanol (B) with a

12 linear gradient of 20–60% B over 25 minutes. Flow rate was maintained at 0.2 ml min^{-1}

13 and the elution was monitored by a diode-array detector (200–600 nm). MRM

14 experiments were conducted at the electrospray ionization interface of an API 2000

15 QTRAP system (Applied Biosystems, H.K.) operating in negative mode. Starch

16 measurement was carried out according to the method of Focks and Benning (1998)

17 using a starch assay kit (Sigma).

18 Enzyme assays

19 Sucrose synthase, soluble invertase and insoluble cell wall invertase activities were

20 measured as described (Xu, *et al.,* 1996; Dejardin *et al.,* 1997). SPS activity was

21 assayed by the anthrone test (Lunn & Furbank, 1997; Baxter *et al.*, 2003). Acid

22 phosphatase activity was assayed by a colorimetric method (Lung *et al.*, 2008) and the

23 total NR activity assay was carried out as described (Yu *et al.*, 1998).

9

1   Pull-down assays using recombinant AtSnRK1.1, AtSnRK1.2, AtGRIK1,

2   AtGRIK2 and 14-3-3 protein

3   Vectors for expressing GST-GRIK1, GST-GRIK2, His-AtSnRK1.1 (a.a. 1–341) and

4   His-AtSnRK1.2 (a.a. 1–342) were gifts from Dr. Shen Wei (Shen *et al.*, 2009). The

5   expression vector GST-BMH1 (containing a yeast 14-3-3 homolog) was a gift from

6   Prof. Carol MacKintosh (University of Dundee, UK). The fusion protein

7   His-AtSnRK1.1/His-AtSnRK1.2 was purified by Ni-NTA beads and the fusion protein

8   GST-GRIK1/GST-GRIK2 by a GST-Trap column (Amersham Biosciences) (Moorhead

9   *et al.*, 1999). For His-AtSnRK1.1/His-AtSnRK1.2 pull-down assays, 20 µg of protein

10 in 200 µl His binding buffer was coupled to 200 µl of Ni-NTA beads and incubated with

11 1 mg total soluble Arabidopsis protein for 2 hr at 4°C. The bound proteins were washed

12 and eluted in binding buffer containing 100 mM imidazole. For the

13 GST-GRIK1/GST-GRIK2 and GST-14-3-3 pull-down assays, 1 mg total plant protein

14 extract was mixed with 5 µg purified GST-fusion protein on 50 µl GST beads with

15 gentle agitation for 2 hr at 4°C. The beads were washed with washing buffer (50 mM

16 HEPES-KOH, pH 7.5, 500 mM NaCl, 1 mM dithiothreitol) five times. Bound proteins

17 were eluted in 50 mM Tris-HCl, pH 8.0, 10 mM reduced glutathione, 500 mM NaCl

18 and subjected to immunoblot analysis.

19 Analysis of proteins in AtPAP2 transgenic Arabidopsis plants

20   Total soluble proteins were extracted according to the trichloroacetic acid method

21 (Zhu *et al.*, 2006). The samples were run in the pH 4–7 range and stained with SYPRO

22 Ruby for total protein staining and Pro-Q Diamond for phosphoprotein staining. Images

23 were analyzed using ImageMaster 2-D Platinum software (GE Healthcare). The target

24 spots were run on a MALDI-TOF/TOF mass spectrometer and identified by peptide

10

1   mass fingerprinting with data searches carried out using MASCOT search tools

2   (http://www.matrixscience.com) in the NCBI non-redundant public protein database.

3   All of the peptide masses were assumed to be monoisotopic and corresponding to

4    $[M^+H^+]$. Carboxymethyl was considered to be a fixed modification, while Oxidation

5   (M), Phospho (ST) and Phospho (Y) were considered variable modifications. The

6   peptide mass tolerance was set at $\pm$ 0.2 Da and the maximum number of missed

7   cleavages was set at one. The identified proteins had more than 5 matched peptides, and

8   the percentage of sequence coverage was greater than 20%. All of the positive protein

9   identification scores were significant (MASCOT score > 60, $P < 0.05$).

10   Metabolomic analysis by ^{1}H-NMR and GC-MS

11   Shoots of 20-day-old Arabidopsis were freeze-dried immediately after harvest. Three

12   biological replicates were used in this study. For ^{1}H-NMR analysis, dried plant tissues

13   (15 mg) were extracted at 50°C with $D_2O:CD_3OD$ (80:20, 1 ml) containing 0.05% (w/v)

14   d_4-TSP (Ward et al., 2003; Beale et al., 2010). NMR data was collected using 128 scans

15   on a Bruker 600 MHz Avance NMR spectrometer (Bruker BioSpin, Coventry, UK)

16   with a water suppression pulse sequence. Data was scaled to an internal standard

17   (d_4-TSP) and binned to regions of equal width (0.01 ppm). For GC-MS analysis,

18   lyophilized plant material (1.00 mg) was mixed with methoxyamine hydrochloride in

19   anhydrous pyridine (50 μL, 16 mg mL^{-1}, containing 40 μg mL^{-1} ribitol) and the samples

20   were heated at 30°C for 90 min with agitation at 550 rpm. MSTFA + 1% TMCS (70 μL)

21   was then added and the sample was heated for 30 minutes at 37°C with agitation at 550

22   rpm. The derivatized samples were equilibrated at room temperature for 2 hr prior to

23   analysis. GC-MS analysis was carried out on a Pegasus III time of flight mass

24   spectrometer (Leco Corp., USA) coupled to an Agilent 6890N gas chromatograph

11

1   (Agilent Technologies) system fitted with a Microseal septum (Merlin Instrument Co.,

2   USA), a FocusLiner port liner (SGE Analytical Science, UK) packed with deactivated

3   quartz wool and a DB-5ms capillary column (15 m x 0.18 mm I.D. x 0.18 μm d.f. with

4   5 m integrated guard column). Data were exported from ChromaTOF software as

5   netCDF files and converted to MassLynx format using the DataBridge module of

6   MassLynx v4.0 software (Waters, UK) for semi-quantification in the QuanLynx

7   module of MassLynx. A unique mass was assigned to each analyte observed in the

8   dataset and its contribution (response factor) to the total ion current of its corresponding

9   mass spectrum determined. For each analyte, peak areas for the unique mass were

10 determined by integration of its corresponding extracted ion chromatogram, and the

11 extracted ion chromatogram areas and response factors were used to calculate a

12 reconstituted TIC peak area. Principal component analysis was carried out using

13 Simca-P v.11 software (Umetrics, Umea) with unit variance scaling. Significance was

14 determined using ANOVA.

15

1   **Results**

2   Identification of a conserved class of PAP, with a C-terminal hydrophobic motif,

3   in photosynthetic eukaryotes

4   AtPAP2 (AT1G13900) was classified as a group IIa PAP, among the 29 AtPAPs (Li *et*

5   *al.*, 2002). The open reading frame of *AtPAP2* encodes a polypeptide of 656 amino

6   acids with a predicted molecular weight of 73.72 kDa and a pI of 6.11. Database

7   searches revealed that the protein contains a metallophosphoesterase domain within

8   amino acids (a.a.) 256–487. In the genomic DNA, *AtPAP2* contains 2 exons. The

9   program TMHMM predicts that AtPAP2 possesses a transmembrane motif at its

10   C-terminus, suggesting that AtPAP2 is a membrane protein.

11   Phylogenetic analysis showed that PAPs with this C-terminal motif could only be

12   found in plants, not in animals (Fig. S1). There are many more PAP-like sequences in

13   the genomes of higher plants than in the genomes of primitive photosynthetic

14   eukaryotes. For instance, there are 29 putative PAP genes in the genome of Arabidopsis

15   (Li *et al.*, 2002) and 2 in *Ostreococcus tauri* (Fig. S1). Unlike Arabidopsis, where two

16   PAPs contain a C-terminal hydrophobic region (AtPAP2 and AtPAP9), only a single

17   PAP-like sequence from other plant genomes was found to carry this additional

18   hydrophobic motif at the C-terminus (Figs. S1, S2 and Table S1). Interestingly, in the

19   genome of the smallest free-living photosynthetic eukaryote, *O. tauri* (Derelle *et al.*,

20   2006), only 2 PAP-like sequences could be found among its 8166 ORFs, of which one

21   (OtPAP2) carries a C-terminal hydrophobic motif (Table S1). In addition to this

22   hydrophobic motif, all the sequences homologous to AtPAP2 carry an acidic a.a.

23   doublet (e.g. EE, DD, ED) in the last 2–8 residues of the polypeptides (Table S1). These

24   findings indicate that PAPs with a C-terminal hydrophobic motif are only found in

13

1 photosynthetic eukaryotes, and have been conserved during the evolution of green

2 plants.

3 ## Expression of AtPAP2 is not affected by phosphorus and sugar treatments

4 To examine the expression pattern of the AtPAP2 protein in various plant organs and

5 at various developmental stages, a polyclonal antiserum was raised against recombinant

6 AtPAP2 protein. A 74 kDa protein was detected in WT Arabidopsis but was absent in

7 the T-DNA insertion line (Fig. S3). This indicates that the antiserum recognizes

8 AtPAP2 specifically. AtPAP2 is highly expressed in siliques, stems, flowers, roots and

9 senescing leaves, but its expression is relatively lower in leaves and mature seeds (Fig.

10 S4). These results corroborate the results from RT-PCR experiments (Zhu *et al.*, 2005).

11 Since AtPAP2 was predicted to be a constitutively expressed protein by spot history

12 analysis (data not shown), the level of AtPAP2 protein expression under various stimuli

13 was examined. As shown in Fig. S5, inorganic phosphate starvation, sucrose, glucose,

14 sorbitol and mannitol treatments did not affect the level of AtPAP2, confirming that its

15 expression is constitutive.

16 ## AtPAP2 overexpression accelerates plant growth and produces higher seed

17 yield

18 A homozygous T-DNA line of *AtPAP2* that carries a T-DNA insertion site in the

19 second exon (1864 bp/1971 bp) was identified (Fig. S3a). The insertion resulted in the

20 loss of AtPAP2 expression, as indicated by the absence of detectable transcript and

21 protein (Fig. S3). Under normal germination conditions on MS agar, the length of

22 hypocotyls of the *AtPAP2* T-DNA insertion line was shorter (~20%–30%) than WT. To

23 confirm whether the disruption of *AtPAP2* was responsible for the phenotype, the

14

1   T-DNA insertion line was complemented by introducing the full-length coding

2   sequence of *AtPAP2* into Arabidopsis under the control of the CaMV 35S promoter.

3   Four homozygous lines were verified by western blot analysis and their hypocotyls

4   were similar to WT seedlings (data not shown). Therefore, AtPAP2 expression indeed

5   rescued the short hypocotyl phenotype of the T-DNA line.

6   Overexpression studies were used to dissect the roles of AtPAP2 *in vivo*. T3

7   homozygous AtPAP2 overexpression (OE) transgenic lines under the control of CaMV

8   35S promoter were generated. Multiple independent lines with increased levels of

9   AtPAP2 protein, as confirmed by western blot analysis, were obtained. Two

10   homozygous lines, OE7 and OE21, were randomly selected for subsequent studies.

11   Compared to WT, both AtPAP2 OE lines displayed earlier bolting (Fig. 1) and

12   produced more lateral branches and inflorescences. Typically, AtPAP2 OE plants

13   started bolting earlier than both WT and the T-DNA line, ~6 days earlier under LD

14   growth conditions and ~14 days earlier under SD conditions (Table 1a). At day 28 (LD)

15   and day 43 (SD), when WT first bolted, AtPAP2 OE lines had produced significantly

16   more cauline leaves and inflorescences than WT (Fig. S6). Conversely, the number of

17   rosette leaves of AtPAP2 OE lines was fewer than WT (Fig. 1b, Table 1a), although the

18   leaf area and total biomass of OE lines were similar to WT at 20-day-old, at day 40, the

19   total leaf area of AtPAP2 OE lines was only 65% that of WT, but the total biomass was

20   2-fold higher than WT (Fig. 1c). AtPAP2 OE plants not only matured earlier but also

21   produced higher seed yields. In two independent experiments, the total seed yield of

22   AtPAP2 OE7 and OE21 plants increased remarkably by 40–57% over WT, which was

23   due to higher numbers of auxiliary branches and a higher silique density (Table 1b). No

24   significant differences in plant growth or seed yield relative to WT were observed in the

25   *AtPAP2* T-DNA line, possibly due to redundancy of gene function.

15

1 AtPAP2 is dual-targeted to chloroplasts and mitochondria

2 The protein sequence of AtPAP2 carries a hydrophobic C-terminal motif (TMD/CT)

3 predicted to carry a trans-membrane motif and it has already been identified as a

4 chloroplast protein by proteomics (Kleffmann *et al.*, 2004). In contrast, the SignalP

5 server predicts that AtPAP2 has a 24 a.a. SP at its N-terminus to direct the protein to the

6 secretory pathway. To investigate the targeting of AtPAP2, 30 a.a. residues from the

7 N-terminus and 69 a.a. residues from the C-terminus were fused to green fluorescent

8 protein (GFP) under the control of the CaMV 35S promoter (Fig. 2a). Red fluorescence

9 protein (RFP) was fused to either the mitochondrial presequence of the ATP synthase

10 F_1-γ subunit from *Nicotiana plumbaginifolia* (F_1–RFP) (Duby *et al.*, 2001) as a

11 mitochondrial targeting marker or to the targeting sequence (a.a. 1–79) of the small

12 subunit of tobacco Rubisco (plastid-mCherry) (Dabney-Smith *et al.*, 1999) as a

13 chloroplast targeting marker. Transient expression of the GFP fusion constructs was

14 performed in WT Arabidopsis PSB-D cell culture (Fig. 2a).

15 Confocal microscopy analysis showed that both GFP (Fig. 2b and c, green) and GFP

16 fused to the N-terminal SP (SP-GFP) (Fig. 2d and e, green) localized to the cytosol, and

17 did not co-localize with the mitochondrial F_1-RFP (Fig. 2b and d, red) or

18 plastid-mCherry (Fig. 2c and e, red) markers. However, GFP constructs containing the

19 TMD/CT region of AtPAP2, including SP-GFP-TMD/CT (Fig. 2f and g) and

20 GFP-TMD/CT (Fig. 2h and i), were targeted to both plastids and to mitochondria,

21 which were also labeled by the MitoTracker Orange (Molecular Probes, USA) (Fig. S7).

22 In addition, the patterns of expression of all GFP constructs were distinct from that of

23 the Golgi marker (RFP-ManI) (Cai *et al.*, 2011), ER marker (RFP-HDEL) (De Caroli *et*

24 *al.*, 2011) (Fig. S8) and peroxisome marker (peroxisome-mCherry) (Nelson *et al.*, 2007)

25 (Fig. S9). These results confirmed the importance of the TMD/CT in dual targeting of

16

1   the reporter GFP protein to mitochondria and plastids, and the TMD/CT alone is

2   sufficient to direct the GFP protein to both organelles.

3   To confirm the subcellular localization of AtPAP2, protein extracts from isolated

4   chloroplasts and mitochondria were probed with the antibody against AtPAP2. A

5   protein band with an apparent molecular mass of 74 kD was detected in both

6   mitochondria and chloroplasts. The purity of the mitochondria and chloroplasts was

7   verified using antibodies raised against a variety of mitochondrial and chloroplast

8   specific proteins (Fig. 2j).

9   C-terminal targeting is crucial for AtPAP2 function

10   To further study the function of the C-terminal motif and the putative signal peptide

11   of AtPAP2, OE lines with AtPAP2 truncation of the C-terminal motif (a.a. 588–656) or

12   its predicted SP (a.a. 1–24) were generated in Arabidopsis by Agrobacterium-mediated

13   plant transformation (Fig. 3). Western blot analysis was employed to verify its

14   overexpression in homozygous transgenic lines.

15   As shown in Fig. 3a, transgenic Arabidopsis lines expressing SP-deleted AtPAP2

16   (P2NS, a.a. 25–656) exhibited phenotypes similar to the full-length AtPAP2 OE lines,

17   such as earlier bolting and higher biomass. In contrast, when the C-terminal motif was

18   deleted, the OE lines (P2NC, a.a. 1–588) grew like the WT Arabidopsis (Fig. 3a). These

19   results suggest that the C-terminal motif of AtPAP2 is critical for its function in

20   Arabidopsis. In contrast, the putative N-terminal signal peptide of AtPAP2 does not

21   seem to be essential.

22   In AtPAP2 OE lines (P2OE and P2NS), two protein bands could be seen in

23   membrane fractions but only the low molecular weight band appeared in the soluble

24   fraction. Furthermore, the high molecular weight protein band was not seen in the

17

1   membrane fraction from the P2NC lines (with no C-terminal motif). Therefore, it is

2   likely that the high molecular weight protein band is a membrane-associated full-length

3   AtPAP2 and the cleavage of its C-terminal motif releases it to the soluble fraction.

4   Correlated with the growth phenotype, the presence of the membrane-associated high

5   molecular weight form is essential to the robust growth phenotypes of the OE lines (Fig.

6   3b).

7   AtPAP2 overexpression changes the carbon metabolism of Arabidopsis

8   Sugars supplied by the shoot are the driving force for plant growth and anabolism.

9   We analyzed the carbohydrate contents of leaves from 20-day-old plants halfway

10   through the light period. The size and morphology of leaves from various lines were

11   still similar at day 20 and therefore this age was chosen for further analysis. Both

12   sucrose and hexose sugar contents were greatly elevated in the shoots of AtPAP2 OE

13   plants (Table 1c), in which sucrose was 1.3- to 1.8-fold and hexose sugars were 1.9- to

14   2.6-fold that of WT ($P<0.01$). However, the starch level did not differ significantly

15   between the various lines (Table 1c).

16   The increased sucrose and hexose sugars (Table 1c) in the AtPAP2 OE plants may be

17   due to altered activity of enzymes involved in sugar metabolism. SPS activity was

18   significantly enhanced in the 20-day-old AtPAP2 OE lines under both optimal V_{max} and

19   limiting V_{limit} conditions, and was not affected by light/dark transitions, as in wild-type

20   Arabidopsis (Huber *et al.*, 1989). In addition, the activities of enzymes involved in

21   sucrose catabolism, including sucrose synthase, acid and alkaline soluble invertase,

22   insoluble cell wall invertases, were unaffected (Table 2). The enzyme activity of acid

23   phosphatase was elevated in both OE lines but the total NR activity was only

24   significantly elevated in one OE line (OE21, Table 2). The higher SPS activity could

1   result from either a higher level of protein expression or a higher activity per enzyme

2   molecule. Western blotting indicated that the SPS protein levels were significantly

3   elevated in the OE lines during both day and night. The levels of the other enzymes,

4   such as fructose-1,6-bisphosphatase (FBPase) and FBP aldolase in the sucrose

5   synthetic pathway did not change significantly (Fig. 4).

6   To investigate whether enhanced SPS activity was due to a change in the relative

7   amounts of phosphorylated SPS versus total SPS, a 14-3-3 capture experiment was

8   carried out. The recombinant 14-3-3 captured similar amounts of phosphorylated SPS

9   in all four lines (Fig. 4). Hence, the increase in SPS activity in the OE lines was due to

10   an increase of the unphosphorylated active form of enzyme. Theoretically, a

11   suppression of SnRK1 kinase activity could enhance SPS activity. Hence, the

12   expression levels of SnRK1 protein subunits and the phosphorylation status of the

13   Thr_{175} residue on its activation loop were examined by western blotting (Fig. S10); the

14   levels of the AtSnRK1.1, AtSnRK β1 and AtSnRK β2 subunits were unaltered. Blots

15   using antiserum against phosphorylated-AMPK (T_{172}), which cross-reacts with

16   phosphorylated Thr_{175} on AtSnRK1 in Arabidopsis (Sugden *et al.*, 1999), indicated that

17   the phosphorylation status of T_{175} was unaltered. This suggested that the higher SPS

18   activity in the OE lines was not mediated by the SnRK1 pathway.

19   Overexpression of AtPAP2 results in alteration of soluble plastid proteins

20   Two-dimensional gel analysis of total leaf soluble proteins revealed that two proteins

21   involved in photosynthesis exhibited changes in the OE lines; first, PSBP-1, an

22   oxygen-evolving enhancer protein (AT1G06680), was induced, and secondly, Rubisco

23   activase (RCA, AT2G39730) showed a mobility shift (Fig. 5). PSBP-1 is required for

24   high levels of oxygen evolution (Mayfield *et al.*, 1987). RCA enhances photosynthetic

19

1   rate by freeing Rubisco for the next round of carbon fixation (Portis, 2003; Portis *et al.*,

2   2008). In Arabidopsis, there are 2 RCA genes (At1g73110 and At2g39730), and

3   alternative splicing of At2g39730 produced 3 isoforms. Deletion of the short

4   thermolabile isoform of At2g39730 (RCA1) caused decreased seed yield while

5   transgenic Arabidopsis overexpressing thermostable RCA1 exhibited higher biomass

6   and photosynthetic rate (Kurek *et al.*, 2007). According to the PhosphAT database

7   (phosphat.mpimp-golm.mpg.de), there is at least one phosphorylation site in both gene

8   products (GLAYDp**T**SDDQ on At2G39730.1; AGGMEp**T**LGKV and

9   VPLIVpTGNDF on AT1G73110). A change in phosphorylation status of RCA

10   conceivably would affect pI, but whether this occurred was not determined.

11   Metabolomic analysis

12   Metabolomic analysis was carried out using a combination of NMR-MS and

13   GC-MS. Shoot samples were collected from 20-day-old plants before bolting. Principal

14   component analysis of ^{1}H-NMR and GS-MS datasets (Fig. S11) was carried out to

15   discern any global changes in the metabolomes of these lines. There was a very clear

16   separation of the OE lines from WT and the T-DNA insertion line by each analytical

17   technique. ^{1}H-NMR was also able to discriminate the T-DNA line from WT samples,

18   although this separation was much smaller. The main changes that could be discerned

19   by ^{1}H-NMR between the T-DNA samples and WT included a reduction in fumarate and

20   citrate levels and several amino acids.

21   Combining the results of metabolomics analysis and LC-MS-MS measurements,

22   metabolites which were increased in the OE lines included alanine, proline, several

23   tricarboxylic acid (TCA) metabolites (citrate, fumarate, malate), sugars (glucose and

24   sucrose) and a metabolite putatively identified as indole acetonitrile, a breakdown

20

1 product of indole glucosinolate. Reduced metabolites in the OE lines included certain

2 amino acids (asparagine, aspartate, glutamine, lysine, methionine, phenylalanine,

3 threonine, tyrosine), GABA, ethanolamine, 4-hydroxybenzoic acid, ribose, phytol,

4 linoleic acid, and linolenic acid (Table S2). In addition, OE lines contained significantly

5 higher levels of putrescine and significantly lower levels of spermidine. The

6 metabolites detected in the glycolysis, TCA and amino acid synthesis pathways are

7 presented in Fig. 6.

8 **Discussion**

9   The genomes of plant species generally contain multiple PAP-like sequences, among

10 which, except Arabidopsis, usually only a single PAP gene carries a C-terminal

11 hydrophobic motif. Amino acid sequence alignment of the 29 PAP-like sequences from

12 the Arabidopsis genome showed that only two AtPAPs (AtPAP2, AT1G13900 and

13 AtPAP9, AT2G03450) carry an additional hydrophobic motif (amino acids 614 to 636

14 of AtPAP2 and amino acids 604 to 626 of AtPAP9) at their C-termini (Table S1), which

15 was predicted as a trans-membrane motif by the TMHMM program. Although AtPAP9

16 shares up to 72% sequence identity with AtPAP2 at protein level, AtPAP9 did not

17 exhibit the biological function of AtPAP2. A homozygous T-DNA line of *AtPAP9*

18 (Salk_129905) and several homozygous AtPAP9 OE lines were identified by genomic

19 PCR and RT-PCR analysis. All of them exhibited normal growth phenotypes, which

20 were very different from that of AtPAP2 OE lines (data not shown). A double T-DNA

21 insertion line of *AtPAP2* and *AtPAP9* was also generated through crossing the pollens of

22 *AtPAP2* insertion line and the pistil of *AtPAP9* insertion line and the interruption of both

23 genes were confirmed by genomic PCR analysis (Fig.S3). The double insertion line

24 exhibited similar phenotypes with that of the *AtPAP2* T-DNA line (data not shown). In

25 addition, two PAP-like sequences could be identified in the genomes of the small

21

1 free-living photosynthetic eukaryotes *O. tauri* (Derelle *et al.*, 2006) and *Micromonas*

2 *pusilla* (Worden *et al.*, 2009), of which only one carries a hydrophobic C-terminal motif.

3 *O. tauri,* belonging to the Prasinophyceae, is the smallest (size < 1 μm) free-living

4 photosynthetic eukaryote known. This unicellular organism lacks a cell wall and each

5 cell carries one chloroplast, one mitochondrion, one Golgi body and a large nucleus.

6 The Prasinophyceae are a primitive group of marine green algae, which suggests an

7 ancient ancestral function of AtPAP2-like proteins in the regulation of carbon

8 partitioning in photosynthetic organisms.

9 In our study, AtPAP2 was shown to be dual-targeted to both chloroplasts and

10 mitochondria, key organelles for two important energy processes in plant cells:

11 photosynthesis and respiration (Nunes-Nesi *et al.*, 2007; Nunes-Nesi *et al.*, 2011). An

12 increasing number of proteins in mitochondria and plastids have been found to be

13 encoded by single nuclear genes, and are referred to as dual-targeted proteins (Peeters

14 & Small, 2001). To date, as many as 47 different proteins from seven plant species have

15 been reported to be dual-targeted (Carrie *et al.*, 2009a). In Arabidopsis, 11 PKs and 10

16 PPs have been shown to be targeted to the chloroplast and all are nuclear encoded

17 (Schliebner *et al.*, 2008; Shapiguzov *et al.*, 2010). In mitochondria, 10 PKs and one PP

18 were identified in Arabidopsis (Heazlewood *et al.*, 2004). All of these PKs and PPs are

19 targeted by N-terminal targeting signals. The identification of a C-terminal

20 dual-targeting signal in AtPAP2 is novel and AtPAP2 is the only PP that is dual-targeted

21 to both organelles.

22 Overexpression of AtPAP2 in Arabidopsis leads to a faster growth rate. The higher

23 biomass but lower total leaf area of 40-day-old transgenic plants provided indirect

24 evidence of a higher photoassimilation rate per leaf area in the OE lines. The changes in

25 RCA and PSBP-1 in the OE lines might also affect the photosynthetic activity of the OE

1   lines. Whether the observed modification of RCA affects the activity of Rubisco and

2   thus results in the enhanced growth rate of AtPAP2 OE lines is an interesting topic for

3   further study.

4   Sucrose is the fuel and building block for sink tissues. AtPAP2 overexpression

5   drastically enhanced the sucrose and hexose levels in rosette leaves while the starch

6   level did not change significantly. SPS activity shows a high correlation with sucrose

7   production in leaves (Baxter *et al.*, 2003; Haigler *et al.*, 2007) and overexpression of

8   SPS promotes earlier flowering, fruit development, and increased biomass in tomato

9   (Micallef *et al.*, 1995) and tobacco (Park *et al.*, 2008). In the two AtPAP2 OE lines, SPS

10 was upregulated at the protein level, which resulted in a significant enhancement of its

11 activity. SnRK1 can phosphorylate and inhibit SPS activity (Halford *et al.*, 2003) under

12 high sucrose levels. Since overexpression of AtSnRK1.1 resulted in phenotypes

13 opposite to that of the AtPAP2 OE plants, such as delayed flowering and retarded

14 growth (Baena-Gonzalez *et al.*, 2007), it may be worth asking whether AtPAP2 is an

15 antagonistic phosphatase of SnRK's kinase activity. Under energy deficiency, activated

16 SnRK1 phosphorylates SPS hence suppresses activity posttranslationally (Toroser *et al.*,

17 1998; Moorhead *et al.*, 1999). In contrast, overexpression of AtPAP2 resulted in higher

18 SPS activity. Theoretically, a phosphatase (Sugden *et al.*, 1999) that specifically

19 dephosphorylates SnRK1 or its upstream kinases (e.g. GRIK) *in vivo* might suppress

20 their biological activity and thus boost the activity of SPS. However, it is unlikely that

21 AtPAP2 mediated its actions through GRIK or SnRK1 because the phosphorylation

22 status of the T_{175} residue was unaltered in the OE lines; also, pull-down experiments

23 only found an interaction between GRIK and SnRK (data not shown), but not between

24 AtPAP2 and GRIK or SnRK1 (Fig. S10). Unlike SnRK1, which inactivates SPS by

25 posttranslational modification, AtPAP2 overexpression enhances sucrose synthesis by

23

1   increasing the expression of SPS.

2   The mechanism of how AtPAP2 stimulates plant growth remains unclear. As the acid

3   phosphatase activity was significantly increased in the AtPAP2 OE lines (Table 2),

4   AtPAP2 may act as a PP or as a phosphatase for inorganic P compounds. In the former

5   scenario, AtPAP2 might exhibit its effects as a PP like PPH1, a chloroplast phosphatase

6   that dephosphorylates light-harvesting complex II during state transition (Finazzi *et al.*,

7   2002; Shapiguzov *et al.*, 2010). In the latter scenario, AtPAP2 might increase the acid

8   phosphatase activity in the chloroplasts and mitochondria, thus releasing more free

9   inorganic phosphate (Pi). In chloroplasts, as Pi is an activator of Rubisco activity,

10   production of triose phosphates might be enhanced by a higher Pi supply (Giersch &

11   Robinson, 1987), and in turn provide more triose phosphate for sucrose synthesis.

12   Similarly, the possibly higher Pi supply in the mitochondrial matrix could also

13   modulate TCA flux and activate oxidative phosphorylation and ATP synthesis (Wu *et*

14   *al.*, 2007). The higher concentrations of fumarate and malate in OE lines (Fig. 6) might

15   reflect a higher flux from succinyl-CoA to succinate (Johnson *et al.*, 1998), another step

16   in the TCA cycle that produces ATP (Meyer *et al.*, 2010). ATP generated from the TCA

17   cycle could be transported out of the mitochondria to sustain the high rate of sucrose

18   synthesis (Kromer *et al.*, 1993). The higher levels of organic acids of the TCA cycle in

19   the OE lines did not result in a higher amino acid level of the aspartate family,

20   indicating that the regulation and the flux of the TCA cycle is a complicated process.

21   Alteration of key enzymes and their activities in the TCA cycle affect photosynthesis:

22   downregulation of aconitase, the iron-sulfur subunit of succinate dehydrogenase and

23   the mitochondrial malate dehydrogenase enhance the rate of photosynthesis (Carrari *et*

24   *al.*, 2003; Nunes-Nesi *et al.*, 2005; Araujo *et al.*, 2011), whereas inhibition of citrate

25   synthase, succinyl CoA ligase, or isocitrate dehydrogenase show little effect on the rate

24

1   (Studart-Guimaraes *et al.*, 2007; Sienkiewicz-Porzucek *et al.*, 2008;

2   Sienkiewicz-Porzucek *et al.*, 2010; Sulpice *et al.*, 2010). All these lines displayed

3   changes in expression levels of organic acids and amino acids. Thus, the mechanism by

4   which AtPAP2 influences both photosynthesis and the TCA cycle is likely to be

5   complex and may be involved in a number of pathways or factors.

6   In summary, we have shown that ectopic overexpression of AtPAP2 in Arabidopsis

7   causes dramatic effects on plant growth and carbon metabolism. Its biological activity

8   is dependent on its dual targeting to both plastids and mitochondria. Whether

9   overexpression of AtPAP can be used as a tool to boost the yield of important crop

10 plants will be an interesting subject of future studies.

11

12 **Supporting Information**

13 **Fig. S1** Phylogenetic analysis of full length AtPAP2 protein sequence with related

14 proteins in the other plant species.

15 **Fig. S2** Amino acid sequence alignment of AtPAP2 with its homologous sequences

16 from other plants.

17 **Fig. S3** Verification of *AtPAP2* T-DNA mutant line.

18 **Fig. S4** Western blot analysis of AtPAP2 in Arabidopsis tissues.

19 **Fig. S5** Expression of AtPAP2 under various treatments.

20 **Fig. S6** Growth phenotypes of genetically modified Arabidopsis.

21 **Fig. S7** The TMD/CT region of AtPAP2 contains targeting signal to mitochondria.

22 **Fig. S8.** AtPAP2-GFP constructs did not co-localize with ER or Golgi markers.

23 **Fig. S9.** AtPAP2-GFP constructs did not co-localize with peroxisome marker**.**

24 **Fig. S10.** Analysis of SnRK1 proteins.

25 **Fig. S11.** Principal Component Analysis of ^{1}H NMR data and GC-MS data.

1   **Table S1.** Signature motifs of AtPAP2-like proteins.

2   **Table S2.** Relative metabolite content of shoots of 20-day-old AtPAP2 OE lines.

3   **Table S3.** Primers used in this study.

4

5   **Acknowledgements**

12

13   **References**

14   **Antonio C, Larson T, Gilday A, Graham I, Bergstroem E, Thomas-Oates J. 2007.**

15   Quantification of sugars and sugar phosphates in *Arabidopsis thaliana* tissues

16   using porous graphitic carbon liquid chromatography-electrospray ionization

17   mass spectrometry. *Journal of Chromatography A* **1172**(2): 170-178.

18   **Antonio C, Larson T, Gilday A, Graham I, Bergstrom E, Thomas-Oates J. 2008.**

19   Hydrophilic interaction chromatography/electrospray mass spectrometry

20   analysis of carbohydrate-related metabolites from *Arabidopsis thaliana* leaf

21   tissue. *Rapid Communications in Mass Spectrometry* **22**(9): 1399-1407.

22   **Araujo WL, Nunes-Nesi A, Osorio S, Usadel B, Fuentes D, Nagy R, Balbo I,**

23   **Lehmann M, Studart-Witkowski C, Tohge T, Martinoia E, Jordana X,**

24   **DaMatta FM, Fernie AR. 2011.** Antisense inhibition of the iron-sulphur

25   subunit of succinate dehydrogenase enhances photosynthesis and growth in

tomato via an organic acid-mediated effect on stomatal aperture. *Plant Cell* **23**(2): 600-627.

Baena-Gonzalez E, Rolland F, Thevelein JM, Sheen J. 2007. A central integrator of transcription networks in plant stress and energy signalling. *Nature* **448**(7156): 938-U910.

Baena-Gonzalez E, Sheen J. 2008. Convergent energy and stress signaling. *Trends in Plant Science* **13**(9): 474-482.

Baxter CJ, Foyer CH, Turner J, Rolfe SA, Quick WP. 2003. Elevated sucrose-phosphate synthase activity in transgenic tobacco sustains photosynthesis in older leaves and alters development. *Journal of Experimental Botany* **54**(389): 1813-1820.

Beale MH, Ward JL, Baker JM, Miller SJ, Deborde C, Maucourt M, Biais B, Rolin D, Moing A, Moco S, Vervoort J, Lommen A, Schafer H, Humpfer E. 2010. An inter-laboratory comparison demonstrates that [(1)H]-NMR metabolite fingerprinting is a robust technique for collaborative plant metabolomic data collection. *Metabolomics* **6**(2): 263-273.

Cai Y, Jia TR, Lam SK, Ding Y, Gao CJ, San MWY, Pimpl P, Jiang LW. 2011. Multiple cytosolic and transmembrane determinants are required for the trafficking of SCAMP1 via an ER-Golgi-TGN-PM pathway. *Plant Journal* **65**(6): 882-896.

Carrari F, Nunes-Nesi A, Gibon Y, Lytovchenko A, Loureiro ME, Fernie AR. 2003. Reduced expression of aconitase results in an enhanced rate of photosynthesis and marked shifts in carbon partitioning in illuminated leaves of wild species tomato. *Plant Physiology* **133**(3): 1322-1335.

Carrie C, Giraud E, Duncan O, Xu L, Wang Y, Huang SB, Clifton R, Murcha M,

Filipovska A, Rackham O, Vrielink A and Whelan J 2010. Conserved and novel functions for *Arabidopsis thaliana* MIA40 in assembly of proteins in mitochondria and peroxisomes. *Journal of Biological Chemistry* **285**(46): 36138-36148.

Carrie C, Giraud E, Whelan J. 2009a. Protein transport in organelles: Dual targeting of proteins to mitochondria and chloroplasts. *The FEBS Journal* **276**(5): 1187-1195.

Carrie C, Kuhn K, Murcha MW, Duncan O, Small ID, O'Toole N, Whelan J. 2009b. Approaches to defining dual-targeted proteins in Arabidopsis. *The Plant Journal : for cell and molecular biology* **57**(6): 1128-1139.

Carrie C, Murcha MW, Kuehn K, Duncan O, Barthet M, Smith PM, Eubel H, Meyer E, Day DA, Millar AH, Whelan J. 2008. Type II NAD(P)H dehydrogenases are targeted to mitochondria and chloroplasts or peroxisomes in *Arabidopsis thaliana*. *FEBS Letters* **582**(20): 3073-3079.

Cashikar AG, Kumaresan R, Rao NM. 1997. Biochemical characterization and subcellular localization of the red kidney bean purple acid phosphatase. *Plant Physiology* **114**(3): 907-915.

Chen S, Songkumarn P, Liu J, Wang GL. 2009. A versatile zero background T-vector system for gene cloning and functional genomics. *Plant Physiology* **150**(3): 1111-1121.

Ciereszko I, Johansson H, Kleczkowski L. 2001. Sucrose and light regulation of a cold-inducible UDP-glucose pyrophosphorylase gene via a hexokinase-independent and abscisic acid-insensitive pathway in Arabidopsis. *Biochemical Journal* **354**(Pt 1): 67.

Clough SJ, Bent AF. 1998. Floral dip: a simplified method for Agrobacterium-

mediated transformation of *Arabidopsis thaliana*. *Plant Journal* **16**(6): 735-743.

Dabney-Smith C, van den Wijngaard PWJ, Treece Y, Vredenberg WJ, Bruce BD. 1999. The C terminus of a chloroplast precursor modulates its interaction with the translocation apparatus and PIRAC. *Journal of Biological Chemistry* **274**(45): 32351-32359.

De Caroli M, Lenucci MS, Di Sansebastiano GP, Dalessandro G, De Lorenzo G, Piro G. 2011. Protein trafficking to the cell wall occurs through mechanisms distinguishable from default sorting in tobacco. *Plant Journal* **65**(2): 295-308.

Dejardin A, Rochat C, Maugenest S, Boutin JP. 1997. Purification, characterization and physiological role of sucrose synthase in the pea seed coat (*Pisum sativum* L). *Planta* **201**(2): 128-137.

del Pozo JC, Allona I, Rubio V, Leyva A, de la Pena A, Aragoncillo C, Paz-Ares J. 1999. A type 5 acid phosphatase gene from *Arabidopsis thaliana* is induced by phosphate starvation and by some other types of phosphate mobilising/oxidative stress conditions. *Plant Journal* **19**(5): 579-589.

Derelle E, Ferraz C, Rombauts S, Rouze P, Worden AZ, Robbens S, Partensky F, Degroeve S, Echeynie S, Cooke R, Saeys Y, Wuyts J, Jabbari K, Bowler C, Panaud O, Piegu B, Ball SG, Ral JP, Bouget FY, Piganeau G, De Baets B, Picard A, Delseny M, Demaille J, Van de Peer Y, Moreau H. 2006. Genome analysis of the smallest free-living eukaryote *Ostreococcus tauri* unveils many unique features. *Proceedings of the National Academy of Sciences of the United States of America* **103**(31): 11647-11652.

Duby G, Oufattole M, Boutry M. 2001. Hydrophobic residues within the predicted N-terminal amphiphilic alpha-helix of a plant mitochondrial targeting

29

presequence play a major role in in vivo import. *Plant Journal* **27**(6): 539-549.

Finazzi G, Rappaport F, Furia A, Fleischmann M, Rochaix JD, Zito F, Forti G. 2002. Involvement of state transitions in the switch between linear and cyclic electron flow in *Chlamydomonas reinhardtii*. *EMBO Reports* **3**(3): 280-285.

Focks N, Benning C. 1998. wrinkled1: A novel, low-seed-oil mutant of Arabidopsis with a deficiency in the seed-specific regulation of carbohydrate metabolism. *Plant Physiology* **118**(1): 91-101.

Gibson SI. 2005. Control of plant development and gene expression by sugar signaling. *Current Opinion in Plant Biology* **8**(1): 93-102.

Giersch C, Robinson SP. 1987. Regulation of photosynthetic carbon metabolism during phosphate limitation of photosynthesis in isolated spinach chloroplasts. *Photosynthesis Research* **14**(3): 211-227.

Haigler CH, Singh B, Zhang DS, Hwang S, Wu CF, Cai WX, Hozain M, Kang W, Kiedaisch B, Strauss RE, Hequet EF, Wyatt BG, Jividen GM, Holaday AS. 2007. Transgenic cotton over-producing spinach sucrose phosphate synthase showed enhanced leaf sucrose synthesis and improved fiber quality under controlled environmental conditions. *Plant Molecular Biology* **63**(6): 815-832.

Halford NG, Hey S, Jhurreea D, Laurie S, McKibbin RS, Paul M, Zhang YH. 2003. Metabolic signalling and carbon partitioning: role of Snf1-related (SnRK1) protein kinase. *Journal of Experimental Botany* **54**(382): 467-475.

Heazlewood JL, Tonti-Filippini JS, Gout AM, Day DA, Whelan J, Millar AH. 2004. Experimental analysis of the Arabidopsis mitochondrial proteome highlights signaling and regulatory components, provides assessment of targeting prediction programs, and indicates plant-specific mitochondrial proteins. *Plant Cell* **16**(1): 241-256.

30

1   **Huber SC, Huber JL, Campbell WH, Redinbaugh MG. 1992.** Apparent

2   dependence of the light activation of nitrate reductase and sucrose phosphate

3   synthase activities in spinach leaves on protein synthesis. *Plant and Cell*

4   *Physiology* **33**(5): 639-646.

5   **Huber SC, Nielsen TH, Huber JLA, Pharr DM. 1989.** Variation among Species in

6   Light Activation of Sucrose-Phosphate Synthase. *Plant and Cell Physiology*

7   **30**(2): 277-285.

8   **Jiang L, Rogers JC. 1998.** Integral membrane protein sorting to vacuoles in plant cells:

9   evidence for two pathways. *Journal of Cell Biology* **143**(5): 1183-1199.

10   **Johnson JD, Mehus JG, Tews K, Milavetz BI, Lambeth DO. 1998.** Genetic

11   evidence for the expression of ATP- and GTP-specific succinyl-CoA

12   synthetases in multicellular eucaryotes. *Journal of Biological Chemistry*

13   **273**(42): 27580-27586.

14   **Kaida R, Satoh Y, Bulone V, Yamada Y, Kaku T, Hayashi T, Kaneko TS. 2009.**

15   Activation of β-glucan synthases by wall bound purple acid phosphatase in

16   tobacco cells. *Plant Physiology* **150**(4): 1822-1830.

17   **Kaida R, Serada S, Norioka N, Norioka S, Neumetzler L, Pauly M, Sampedro J,**

18   **Zarra I, Hayashi T, Kaneko TS. 2010.** Potential role for purple acid

19   phosphatase in the dephosphorylation of wall proteins in tobacco cells. *Plant*

20   *Physiology* **153**(2): 603-610.

21   **Kleffmann T, Russenberger D, von Zychlinski A, Christopher W, Sjolander K,**

22   **Gruissem W, Baginsky S. 2004.** The *Arabidopsis thaliana* chloroplast

23   proteome reveals pathway abundance and novel protein functions. *Current*

24   *Biology* **14**(5): 354-362.

25   **Kromer S, Malmberg G, Gardestrom P. 1993.** Mitochondrial contribution to

31

photosynthetic metabolism (A study with barley (*Hordeum vulgare* L.) leaf protoplasts at different light intensities and CO_2 concentrations). *Plant Physiology* **102**(3): 947-955.

Kuang R, Chan KH, Yeung E, Lim BL. 2009. Molecular and biochemical characterization of AtPAP15, a purple acid phosphatase with phytase activity, in Arabidopsis. *Plant Physiology* **151**(1): 199-209.

Kubis SE, Lilley KS, Jarvis P. 2008. Isolation and preparation of chloroplasts from *Arabidopsis thaliana* plants. *Methods in Molecular Biology* **425**: 171-186.

Kumar S, Tamura K, Nei M. 2004. MEGA3: Integrated software for molecular evolutionary genetics analysis and sequence alignment. *Briefings in Bioinformatics* **5**(2): 150-163.

Kurek I, Chang TK, Bertain SM, Madrigal A, Liu L, Lassner MW, Zhu G. 2007. Enhanced Thermostability of Arabidopsis Rubisco activase improves photosynthesis and growth rates under moderate heat stress. *Plant Cell* **19**(10): 3230-3241.

Li D, Zhu H, Liu K, Liu X, Leggewie G, Udvardi M, Wang D. 2002. Purple acid phosphatases of *Arabidopsis thaliana*. Comparative analysis and differential regulation by phosphate deprivation. *Journal of Biological Chemistry* **277**(31): 27772-27781.

Li WYF, Shao G, Lam HM. 2008. Ectopic expression of GmPAP3 alleviates oxidative damage caused by salinity and osmotic stresses. *New Phytologist* **178**(1): 80-91.

Liao H, Wong FL, Phang TH, Cheung MY, Li WY, Shao G, Yan X, Lam HM. 2003. GmPAP3, a novel purple acid phosphatase-like gene in soybean induced by NaCl stress but not phosphorus deficiency. *Gene* **318**: 103-111.

32

1 **Lister R, Carrie C, Duncan O, Ho LH, Howell KA, Murcha MW, Whelan J. 2007.**

2   Functional definition of outer membrane proteins involved in preprotein import

3   into mitochondria. *The Plant cell* **19**(11): 3739-3759.

4 **Lung SC, Leung A, Kuang R, Wang Y, Leung P, Lim BL. 2008.** Phytase activity in

5   tobacco (*Nicotiana tabacum*) root exudates is exhibited by a purple acid

6   phosphatase. *Phytochemistry* **69**(2): 365-373.

7 **Lunn JE, Furbank RT. 1997.** Localisation of sucrose-phosphate synthase and starch

8   in leaves of C4 plants. *Planta* **202**(1): 106-111.

9 **Lunn JE, MacRae E. 2003.** New complexities in the synthesis of sucrose. *Currunt*

10   *Opinion in Plant Biology* **6**(3): 208-214.

11 **Martinez-Noel GM, Tognetti JA, Salerno GL, Wiemken A, Pontis HG. 2009.**

12   Protein phosphatase activity and sucrose-mediated induction of fructan

13   synthesis in wheat. *Planta* **230**(5): 1071-1079.

14 **Mayfield SP, Rahire M, Frank G, Zuber H, Rochaix JD. 1987.** Expression of the

15   nuclear gene encoding oxygen-evolving enhancer protein 2 Is required for high

16   levels of photosynthetic oxygen evolution in *Chlamydomonas reinhardtii*.

17   *Proceedings of the National Academy of Sciences of the United States of*

18   *America* **84**(3): 749-753.

19 **Meyer S, De Angeli A, Fernie AR, Martinoia E. 2010.** Intra- and extra-cellular

20   excretion of carboxylates. *Trends in Plant Science* **15**(1): 40-47.

21 **Miao Y, Jiang L. 2007.** Transient expression of fluorescent fusion proteins in

22   protoplasts of suspension cultured cells. *Nature Protococols* **2**(10): 2348-2353.

23 **Micallef B, Haskins K, Vanderveer P, Roh K, Shewmaker C, Sharkey T. 1995.**

24   Altered photosynthesis, flowering, and fruiting in transgenic tomato plants that

25   have an increased capacity for sucrose synthesis. *Planta* **196**(2): 327-334.

1 **Moorhead G, Douglas P, Cotelle V, Harthill J, Morrice N, Meek S, Deiting U, Stitt**

2 **M, Scarabel M, Aitken A, MacKintosh C. 1999.** Phosphorylation-dependent

3 interactions between enzymes of plant metabolism and 14-3-3 proteins. *Plant*

4 *Journal* **18**(1): 1-12.

5 **Nelson BK, Cai X, Nebenfuhr A. 2007.** A multicolored set of in vivo organelle

6 markers for co-localization studies in Arabidopsis and other plants. *Plant*

7 *Journal* **51**(6): 1126-1136.

8 **Nunes-Nesi A, Araujo WL, Fernie AR. 2011.** Targeting mitochondrial metabolism

9 and machinery as a means to enhance photosynthesis. *Plant Physiology* **155**(1):

10 101-107.

11 **Nunes-Nesi A, Carrari F, Lytovchenko A, Smith AMO, Loureiro ME, Ratcliffe**

12 **RG, Sweetlove LJ, Fernie AR. 2005.** Enhanced photosynthetic performance

13 and growth as a consequence of decreasing mitochondrial malate

14 dehydrogenase activity in transgenic tomato plants. *Plant Physiology* **137**(2):

15 611-622.

16 **Nunes-Nesi A, Sweetlove LJ, Fernie AR. 2007.** Operation and function of the

17 tricarboxylic acid cycle in the illuminated leaf. *Physiologia Plantarum* **129**(1):

18 45-56.

19 **Park AY, Canam T, Kang KY, Ellis DD, Mansfield SD. 2008.** Over-expression of

20 an Arabidopsis family A sucrose phosphate synthase (SPS) gene alters plant

21 growth and fibre development. *Transgenic Research* **17**(2): 181-192.

22 **Peeters N, Small I. 2001.** Dual targeting to mitochondria and chloroplasts. *Biochimica*

23 *Et Biophysica Acta-Molecular Cell Research* **1541**(1-2): 54-63.

24 **Polge C, Jossier M, Crozet P, Gissot L, Thomas M. 2008.** Beta-subunits of the

25 SnRK1 complexes share a common ancestral function together with expression

34

and function specificities; physical interaction with nitrate reductase specifically occurs via AKINbeta1-subunit. *Plant Physiology* **148**(3): 1570-1582.

Portis AR. 2003. Rubisco activase - Rubisco's catalytic chaperone. *Photosynthesis Research* **75**(1): 11-27.

Portis AR, Jr., Li C, Wang D, Salvucci ME. 2008. Regulation of Rubisco activase and its interaction with Rubisco. *Journal of Experimental Botany* **59**(7): 1597-1604.

Rolland F, Baena-Gonzalez E, Sheen J. 2006. Sugar sensing and signaling in plants: Conserved and novel mechanisms. *Annual Review of Plant Biology* **57**: 675-709.

Rolland F, Moore B, Sheen J. 2002. Sugar sensing and signaling in plants. *Plant Cell* **14**: S185-S205.

Saitou N, Nei M. 1987. The neighbor-joining method: a new method for reconstructing phylogenetic trees. *Molecular Biology and Evolution* **4**(4): 406-425.

Schenk G, Guddat LT, Ge Y, Carrington LE, Hume DA, Hamilton S, de Jersey J. 2000. Identification of mammalian-like purple acid phosphatases in a wide range of plants. *Gene* **250**(1-2): 117-125.

Schliebner I, Pribil M, Zuhlke J, Dietzmann A, Leister D. 2008. A survey of chloroplast protein kinases and phosphatases in *Arabidopsis thaliana*. *Current Genomics* **9**(3): 184-190.

Shapiguzov A, Ingelsson B, Samol I, Andres C, Kessler F, Rochaix JD, Vener AV, Goldschmidt-Clermont M. 2010. The PPH1 phosphatase is specifically involved in LHCII dephosphorylation and state transitions in Arabidopsis. *Proceedings of the National Academy of Sciences of the United States of*

35

America **107**(10): 4782-4787.

Sharma-Natu P, Ghildiyal M. 2005. Potential targets for improving photosynthesis and crop yield. *Current Science* **88**(1918): 1928.

Shen W, Hanley-Bowdoin L. 2006. Geminivirus infection up-regulates the expression of two Arabidopsis protein kinases related to yeast SNF1-and mammalian AMPK-activating kinases. *Plant Physiology* **142**(4): 1642-1655.

Shen W, Reyes MI, Hanley-Bowdoin L. 2009. Arabidopsis protein kinases GRIK1 and GRIK2 specifically activate SnRK1 by phosphorylating its activation loop. *Plant Physiology* **150**(2): 996-1005.

Siedlecka A, Ciereszko I, Mellerowicz E, Martz F, Chen J, Kleczkowski L. 2003. The small subunit ADP-glucose pyrophosphorylase (ApS) promoter mediates okadaic acid-sensitive uidA expression in starch-synthesizing tissues and cells in Arabidopsis. *Planta* **217**(2): 184-192.

Sienkiewicz-Porzucek A, Nunes-Nesi A, Sulpice R, Lisec J, Centeno DC, Carillo P, Leisse A, Urbanczyk-Wochniak E, Fernie AR. 2008. Mild reductions in mitochondrial citrate synthase activity result in a compromised nitrate assimilation and reduced leaf pigmentation but have no effect on photosynthetic performance or growth. *Plant Physiology* **147**(1): 115-127.

Sienkiewicz-Porzucek A, Sulpice R, Osorio S, Krahnert I, Leisse A, Urbanczyk-Wochniak E, Hodges M, Fernie AR, Nunes-Nesi A. 2010. Mild reductions in mitochondrial NAD-dependent Isocitrate dehydrogenase activity result in altered nitrate assimilation and pigmentation but do not impact growth. *Molecular Plant* **3**(1): 156-173.

Smeekens S, Ma J, Hanson J, Rolland F. 2010. Sugar signals and molecular networks controlling plant growth. *Currunt Opinion in Plant Biology* **13**(3):

36

1   274-279.

2   **Studart-Guimaraes C, Fait A, Nunes-Nesi A, Carrari F, Usadel B, Fernie AR.**

3   **2007.** Reduced expression of succinyl-coenzyme A ligase can be compensated

4   for by up-regulation of the gamma-aminobutyrate shunt in illuminated tomato

5   leaves. *Plant Physiology* **145**(3): 626-639.

6   **Sugden C, Crawford RM, Halford NG, Hardie DG. 1999.** Regulation of spinach

7   SNF1-related (SnRK1) kinases by protein kinases and phosphatases is

8   associated with phosphorylation of the T loop and is regulated by 5 '-AMP.

9   *Plant Journal* **19**(4): 433-439.

10   **Sulpice R, Sienkiewicz-Porzucek A, Osorio S, Krahnert I, Stitt M, Fernie AR,**

11   **Nunes-Nesi A. 2010.** Mild reductions in cytosolic NADP-dependent isocitrate

12   dehydrogenase activity result in lower amino acid contents and pigmentation

13   without impacting growth. *Amino Acids* **39**(4): 1055-1066.

14   **Takeda S, Mano S, Ohto M, Nakamura K. 1994.** Inhibitors of protein phosphatases 1

15   and 2A block the sugar-inducible gene expression in plants. *Plant Physiology*

16   **106**(2): 567.

17   **Toroser D, Athwal GS, Huber SC. 1998.** Site-specific regulatory interaction between

18   spinach leaf sucrose-phosphate synthase and 14-3-3 proteins. *FEBS Letters*

19   **435**(1): 110-114.

20   **Tse YC, Mo B, Hillmer S, Zhao M, Lo SW, Robinson DG, Jiang L. 2004.**

21   Identification of multivesicular bodies as prevacuolar compartments in

22   *Nicotiana tabacum* BY-2 cells. *Plant Cell* **16**(3): 672-693.

23   **Ward JL, Harris C, Lewis J, Beale MH. 2003.** Assessment of 1H NMR spectroscopy

24   and multivariate analysis as a technique for metabolite fingerprinting of

25   *Arabidopsis thaliana*. *Phytochemistry* **62**(6): 949-957.

37

Winter H, Huber J, Huber S. 1997. Membrane association of sucrose synthase: changes during the graviresponse and possible control by protein phosphorylation. *FEBS Letters* **420**(2-3): 151-155.

Worden AZ, Lee JH, Mock T, Rouze P, Simmons MP, Aerts AL, Allen AE, Cuvelier ML, Derelle E, Everett MV, Foulon E, Grimwood J, Gundlach H, Henrissat B, Napoli C, McDonald SM, Parker MS, Rombauts S, Salamov A, Von Dassow P, Badger JH, Coutinho PM, Demir E, Dubchak I, Gentemann C, Eikrem W, Gready JE, John U, Lanier W, Lindquist EA, Lucas S, Mayer KF, Moreau H, Not F, Otillar R, Panaud O, Pangilinan J, Paulsen I, Piegu B, Poliakov A, Robbens S, Schmutz J, Toulza E, Wyss T, Zelensky A, Zhou K, Armbrust EV, Bhattacharya D, Goodenough UW, Van de Peer Y, Grigoriev IV. 2009. Green evolution and dynamic adaptations revealed by genomes of the marine picoeukaryotes Micromonas. *Science* **324**(5924): 268-272.

Wu F, Yang F, Vinnakota KC, Beard DA. 2007. Computer modeling of mitochondrial tricarboxylic acid cycle, oxidative phosphorylation, metabolite transport, and electrophysiology. *Journal of Biological Chemistry* **282**(34): 24525-24537. D. R. and K. E. Koch

Xu J, Avigne WT, McCarty DR, Koch KE. 1996. A similar dichotomy of sugar modulation and developmental expression affects both paths of sucrose metabolism: Evidence from a maize invertase gene family." *Plant Cell* **8**(7): 1209-1220.

Yu XD, Sukumaran S, Marton L. 1998. Differential expression of the Arabidopsis Nia1 and Nia2 genes - Cytokinin-induced nitrate reductase activity is correlated with increased Nia1 transcription and mRNA levels. *Plant Physiology* **116**(3):

1   1091-1096.

2   **Zheng Z, Xu X, Crosley RA, Greenwalt SA, Sun Y, Blakeslee B, Wang L, Ni W,**

3   **Sopko MS, Yao C, Yau K, Burton S, Zhuang M, McCaskill DG, Gachotte**

4   **D, Thompson M, Greene TW. 2010.** The protein kinase SnRK2.6 mediates

5   the regulation of sucrose metabolism and plant growth in Arabidopsis. *Plant*

6   *Physiology* **153**(1): 99-113.

7   **Zhu HF, Qian WQ, Lu XZ, Li DP, Liu X, Liu KF, Wang DW. 2005.** Expression

8   patterns of purple acid phosphatase genes in Arabidopsis organs and functional

9   analysis of AtPAP23 predominantly transcribed in flower. *Plant Molecular*

10   *Biology* **59**(4): 581-594.

11   **Zhu JM, Chen SX, Alvarez S, Asirvatham VS, Schachtman DP, Wu YJ, Sharp**

12   **RE. 2006.** Cell wall proteome in the maize primary root elongation zone. I.

13   Extraction and identification of water-soluble and lightly ionically bound

14   proteins. *Plant Physiology* **140**(1): 311-325.

15

16   **Figure Legends**

17   **Fig. 1** Growth phenotypes of AtPAP2 overexpression (OE) and T-DNA inactivation

18   Arabidopsis lines. (a) 4-week-old plants grown under LD conditions. (b) Leaves at day

19   27 under LD conditions. (c) Dry weight and total leaf area of 40-day-old plants.

20   AtPAP2 OE lines exhibited higher biomass but much lower leaf area at 40 days of age.

21   Leaves were cut (including leaves on inflorescences, if any) and scanned. The leaf area

22   was calculated using Metamorph (www.image1.com). The dry weights of individual

23   plant samples (including leaves) were measured after water evaporation by heat. The

24   experiments were repeated at least 3 times.

25

39

1 **Fig. 2 AtPAP2 protein is targeted to both mitochondria and chloroplasts.** (a)

2 Targeting of GFP fusion proteins in Arabidopsis PSB-D protoplasts. Transient

3 expression in Arabidopsis PSB-D protoplasts showed that GFP (GFP only) (b, c) and

4 GFP fused with the putative SP region of AtPAP2 (SP-GFP) (d, e) were directed to the

5 cytosol, whereas GFP constructs fused with the TMD/CT region of AtPAP2, including

6 SP-GFP-TMD/CT (f, g) and GFP-TMD/CT (h, i), co-localized with mitochondrial

7 (F1-RFP) and chloroplastic (plastid-mCherry) markers. Bar = 50 μm. Western blot of

8 AtPAP2 protein in mitochondria and chloroplasts. (j) Isolated mitochondria and

9 chloroplasts from 10-day-old seedlings were analyzed by western blotting for the

10 presence of AtPAP2. Purity of the isolated organelles was determined by blotting with

11 antibodies specific to each organelle. Mitochondria: Cytochrome oxidase subunit II

12 (CoxII), the Rieske iron sulfur cluster binding protein (Risp) and translocase of the

13 outer membrane protein of 40 kDa (Tom40). Chloroplasts: Rubisco large subunit and

14 Rubisco small subunit (SSU).

15

16 **Fig. 3** AtPAP2 sublocalization in transgenic plants. (a) Phenotype of 40-day-old plants

17 (n = 12) of WT, P2NS (a.a. 25–656), OE7 (a.a. 1–656), P2NC (a.a. 1–588) and *AtPAP2*

18 T-DNA plants. (b) AtPAP2 protein band identification in WT, P2NS, OE7, P2NC and

19 *AtPAP2* T-DNA plants by western blot analysis.

20

21 **Fig. 4** Western blotting of enzymes involved in sucrose biosynthesis**.** Total soluble

22 protein (30 μg) extracted from the shoots of 20-day-old Arabidopsis was loaded to each

23 lane and was analyzed by western blotting using anti-SPS, anti-FBP aldolase and

24 anti-cFBPase antibodies (Agrisera, Sweden). The pulled-down eluates of GST-14-3-3

25 were diluted 1:1 with 40 μl SDS sample buffer and half was loaded into each lane.

1

2 **Fig. 5** Analysis of protein from AtPAP2 OE lines. An equal volume of total soluble

3 protein (300 μg) extracted from 20-day-old Arabidopsis was analyzed by 2-D gel

4 electrophoresis. Gels were stained with Pro-Q Diamond and SYPRO Ruby. The pI

5 range of the gel was 4-7. Targeted spots are identified by the arrows. Mobility shifts of

6 Rubisco activase (RCA) and oxygen-evolving enhancer protein (PSBP-1) are indicated

7 by the arrows. Three biological replicates were used in this study.

8

9 **Fig. 6** Altered metabolites in 20-day-old AtPAP2 OE lines. Metabolites in red and blue

10 indicate increased or decreased levels, respectively, in AtPAP2 OE plants. Metabolites

11 in black were not detected and those in green were unaltered. The dashed blue circles

12 represent the Asp-family and aromatic amino acid network. DHAP, dihydroxyacetone

13 phosphate; GABA, γ-aminobutyric acid; SA, salicylic acid; DC-SAM, decarboxylated

14 S-adenosylmethionine.

15

16 **Fig. S1** Phylogenetic analysis of the full-length AtPAP2 protein sequence with related

17 proteins in other plant species.

18 The phylogenetic tree was constructed by MEGA 4.1 software based on the

19 neighbor-joining method (Kumar *et al.*, 2004). Scale bar represents 0.2 substitutions

20 per site. The first two letters of each protein represent the abbreviated species name

21 from which they are derived: At: *Arabidopsis thaliana* (AtPAP9, AAM15910; 72%); Br:

22 *Brassica rapa* subsp. *Pekinensis* (AC176823; 84%); Hv: *Hordeum vulgare*

23 (PUT-161a-Hordeum_vulgare-1024109806, 56%); Mt: *Medicago truncatula*

24 (AC202582; 60%); Os: *Oriza sativa* (NM_001065273; 57%); Pp: *Physcomitrella*

25 *patens* subsp. *patens* (XM_001768668.1, 46%); Pt: *Poplar trichocarpa* (NC_008476.1;

41

1   57%); St: *Solanum tuberosum* (PUT-157a-Solanum_tuberosum-29226, 60%); Zm: *Zea*

2   *mays* (ACG47621; 58%); MpPAP1: *Micromonas pusilla* (XP_003057348); MpPAP2:

3   *M. pusilla* (EEH53803, 25%); OtPAP1: *Ostreococcus tauri* (XM_003079445); OtPAP2:

4   *O.s tauri* (XP_003075106; 29%).

5

6   **Fig. S2** Amino acid sequence alignment of AtPAP2 with homologous sequences from

7   other plants. The full-length amino acid sequence of AtPAP2 was aligned to

8   homologous sequences from *Arabidopsis thaliana, Brassica rapa, Ostreococcus tauri*

9   and AtPAP15, which does not carry the C-terminal hydrophobic motif (Kuang *et al.*,

10 2009), with CLC Sequence Viewer 6 software. All five of the conserved domains (in

11 blue) and the seven invariable residues (indicated by an asterisk) of the PAP

12 metal-ligating residues were conserved among PAPs. The pink box indicates the

13 predicted signal peptide of AtPAP2. Hydrophobic motifs at the C-termini of these

14 polypeptides are underlined in red.

15

16 **Fig. S3** Verification of *AtPAP2* T-DNA mutant line.

17 (a) Schematic map showing the location of the T-DNA insertion in *AtPAP2* (second

18 exon, Col ecotype, Salk_013567). (b) Genomic PCR screening for homozygous

19 *AtPAP2* T-DNA line. Primers (LBa and RP2) in the T-DNA and its flanking sequence

20 are indicated. (c) RT-PCR of the *AtPAP2* T-DNA line using full-length AtPAP2 primers

21 P2YF and P2NR. Elongation factor (*EF*) was employed as a control. (d) Western blot

22 analysis of *AtPAP2* T-DNA line using AtPAP2-specific antibody. Coomassie Blue

23 protein staining was used as a loading control. (e) Genomic PCR screening for *AtPAP2*

24 and *AtPAP9* double mutant. Primers employed for amplifying wild type *AtPAP2* and its

25 T-DNA insertion were LP2 + RP2 (A) and LBa + RP2 (B), respectively. Primers

1   employed for amplifying wild type *AtPAP9* and its T-DNA insertion were LP9 + RP9

2   (C) and LBa + RP9 (D), respectively.

3

4   **Fig. S4** Western blot analysis of AtPAP2 in Arabidopsis tissues. Ten-day-old seedlings

5   were germinated and grown on MS agar plates. Mature tissues and senescent leaves

6   were collected from 5- to 6-week-old plants. Equal amounts of total protein (30 µg per

7   lane) were loaded into each lane. Se, dry seeds; SL, senescent leaves; L mature leaves;

8   St, stems; Si, siliques; Fl: flowers; R, roots; YS: young seedlings. Two independent

9   experiments generated the same results.

10

11   **Fig. S5** Expression of AtPAP2 following various treatments.

12   Five-day-old seedlings of WT Arabidopsis were transferred to Pi starvation conditions

13   and MS media containing different concentrations of sugars. Total soluble protein (30

14   µg) was extracted and loaded for western blot analysis using anti-AtPAP2 antibody. (a)

15   Seedlings germinated in Pi starvation medium were transferred to Pi-sufficient MS

16   medium for 2, 4, 7, or 10 days. (b) Seedlings germinated under Pi-sufficient MS

17   medium were transferred to Pi starvation medium for 0, 2, 4, 6, or 8 days. Cytosolic

18   marker protein FBPase was selected as the internal control. Seedlings were treated with

19   sucrose (c), glucose (e), sorbitol (d) and mannitol (f) gradients (% w/v) for 24 hr. At

20   least 3 independent experiments were performed.

21

22   **Fig. S6** Growth phenotypes of genetically modified Arabidopsis.

23   Bolting statistics of 4 lines in LD and SD growth conditions. Number of rosette leaves

24   (a, d), inflorescences (b, e) and cauline leaves (c, f). (n = 10–15).

25

43

1   **Fig. S7** The TMD/CT region of AtPAP2 contains a targeting signal to mitochondria.

2   Transient expression in Arabidopsis PSB-D protoplasts showed that GFP without any

3   targeting sequence (GFP only; a) and GFP with the putative SP region of AtPAP2

4   (SP-GFP; b) were localized in the cytosol and were distinct from mitochondria. GFP

5   constructs containing the TMD/CT region of AtPAP2, including SP-GFP-TMD/CT (c)

6   and GFP-TMD/CT (d), were both targeted to mitochondria and co-localized with

7   mitochondrial marker MitoTracker Orange (red). Bar = 50 µm.

8

9   **Fig. S8** AtPAP2-GFP constructs did not co-localize with ER or Golgi markers.

10   Transient expression in Arabidopsis PSB-D protoplasts showed that SP-GFP (a, d),

11   SP-GFP-TMD/CT (b, e) and GFP-TMD/CT (c, f) did not co-localize with an ER

12   marker (RFP-HDEL; a–c) or Golgi marker (RFP-ManI; d–f). Bar = 50 µm.

13

14   **Fig. S9** AtPAP2-GFP constructs did not co-localize with a peroxisome marker**.**

15   Transient expression in Arabidopsis PSB-D protoplasts showed that GFP only (a),

16   SP-GFP (b), SP-GFP-TMD/CT (c) and GFP-TMD/CT (d) did not co-localize with a

17   peroxisome marker (peroxisome-mCherry, red). Bar = 50 µm.

18

19   **Fig. S10** Analysis of SnRK1 proteins. (a) Western blotting analysis. Samples were

20   collected from 20-day-old Arabidopsis in the middle of the day and the middle of the

21   night. The total soluble protein was separated by SDS-PAGE and immunodetected with

22   anti-SnRK1.1, anti-AMPKT$_{172}$ (Cell Signaling Technology, USA), anti-SnRKβ1

23   (anti-AKINβ1，Agrisera, Sweden) and anti-SnRKβ2 (anti-AKINβ2, Agrisera, Sweden)

24   antibodies. Anti-cFBPase was used as a marker for loading controls. (b) *In vitro*

25   pull-down assays. AtSnRK1/AtSnRK1.2 (SnRK1.1/SnRK1.2) and its upstream kinase,

44

1   GST-AtGRIK1/GST-AtGRIK2 (GRIK1/ GRIK2), did not interact with AtPAP2.

2

3   **Fig. S11** Principal component analysis of ^{1}H NMR data (a) and GC-MS data (b). The

4   shoots of 20-day-old Arabidopsis were used for metabolomic analysis. Three biological

5   replicates per line were used in this study.

6

45

1 **Table 1.** Growth phenotypes of transgenic Arabidopsis. Seeds of WT, T-DNA line and

2 two AtPAP2 OE lines (OE7 and OE21) were germinated in the MS agar for 10 days,

3 seedlings with the same size were transferred to a growth chamber. Statistically

4 differences ($p < 0.05$) in the same row for each line were based on one-way analysis of

5 variance (ANOVA) analysis followed by Tukey's Honestly Significant Differences

6 (HSD) test using statistical program SPSS 11.5. There are 8-15 replicates for each line.

7 The data were reproducible in at least 2 independent experiments.

8 (a) Bolting time

Lines	Long Day (16h/8h)		Short Day (8h/16h)	
	AEI	NRL	AEI	NRL
WT	26.9 ± 1.2^a	13.0 ± 0.8^a	41.0 ± 4.7^a	18.0 ± 3.0^a
T-DNA	25.7 ± 0.7^a	11.6 ± 1.1^a	40.7 ± 4.9^a	15.0 ± 3.0^a
OE7	20.0 ± 1.1^b	6.4 ± 0.5^b	25.6 ± 1.3^b	5.3 ± 0.5^b
OE21	20.8 ± 0.6^b	6.5 ± 0.7^b	26.0 ± 1.1^b	5.4 ± 0.5^b

AEI: Average date of emergence of inflorescence
NRL: No. of rosette leaves at the first appearance of inflorescence

9 (b) Seed yield at maturity.

Lines	No. of Siliques/plant	Seed Yield (g/plant)	Seed weight (mg/100seeds)
WT	396 ± 89^a	0.225 ± 0.058^a	1.96 ± 0.14^a
T-DNA	386 ± 70^a	0.240 ± 0.049^a	2.02 ± 0.16^a
OE7	621 ± 76^b	0.351 ± 0.050^b	1.91 ± 0.10^a
OE21	625 ± 94^b	0.355 ± 0.066^b	1.98 ± 0.03^a

10 All seeds and siliques from a single plant were harvested after the plant was completely

11 dried. The plants were grown under LD regime.

12

13 (c) Carbohydrate contents in 20-day-old Arabidopsis shoots.

	Sucrose (µg/g FW)	Hexose (µg/g FW)	Starch (mg/g FW)
WT	110.1 ± 33.3^a	16.7 ± 7.1^a	3.3 ± 0.4^a
T-DNA	116.1 ± 15.6^a	24.9 ± 7.3^a	4.4 ± 1.1^a
OE7	207.1 ± 22.5^b	43.9 ± 9.2^b	3.8 ± 1.0^a
OE21	147.7 ± 17.3^c	31.7 ± 4.8^{ac}	3.5 ± 0.8^a

14 Sugars were extracted 8 hours after illumination during the LD regime from 20-day-old

15 Arabidopsis.

46

Table 2. Enzyme assays. Samples were collected 8 hours after the light period (Day) and 4 hours after the dark period (Night). Values set in bold type marked with a different letter were determined by the *t* test to be significantly from WT and were determined by the ANOVA-Turkey test to be significantly different ($p < 0.05$) from each other. There are 3 biological replicates in this study.

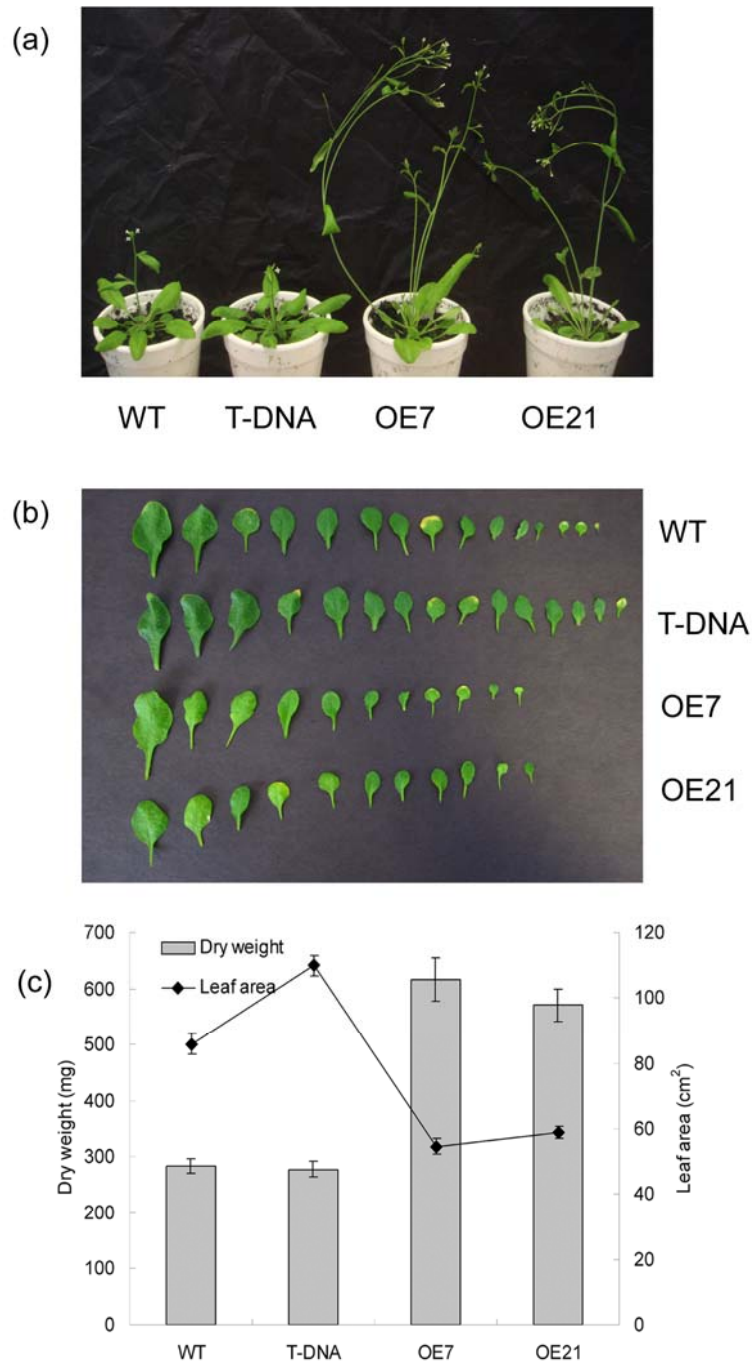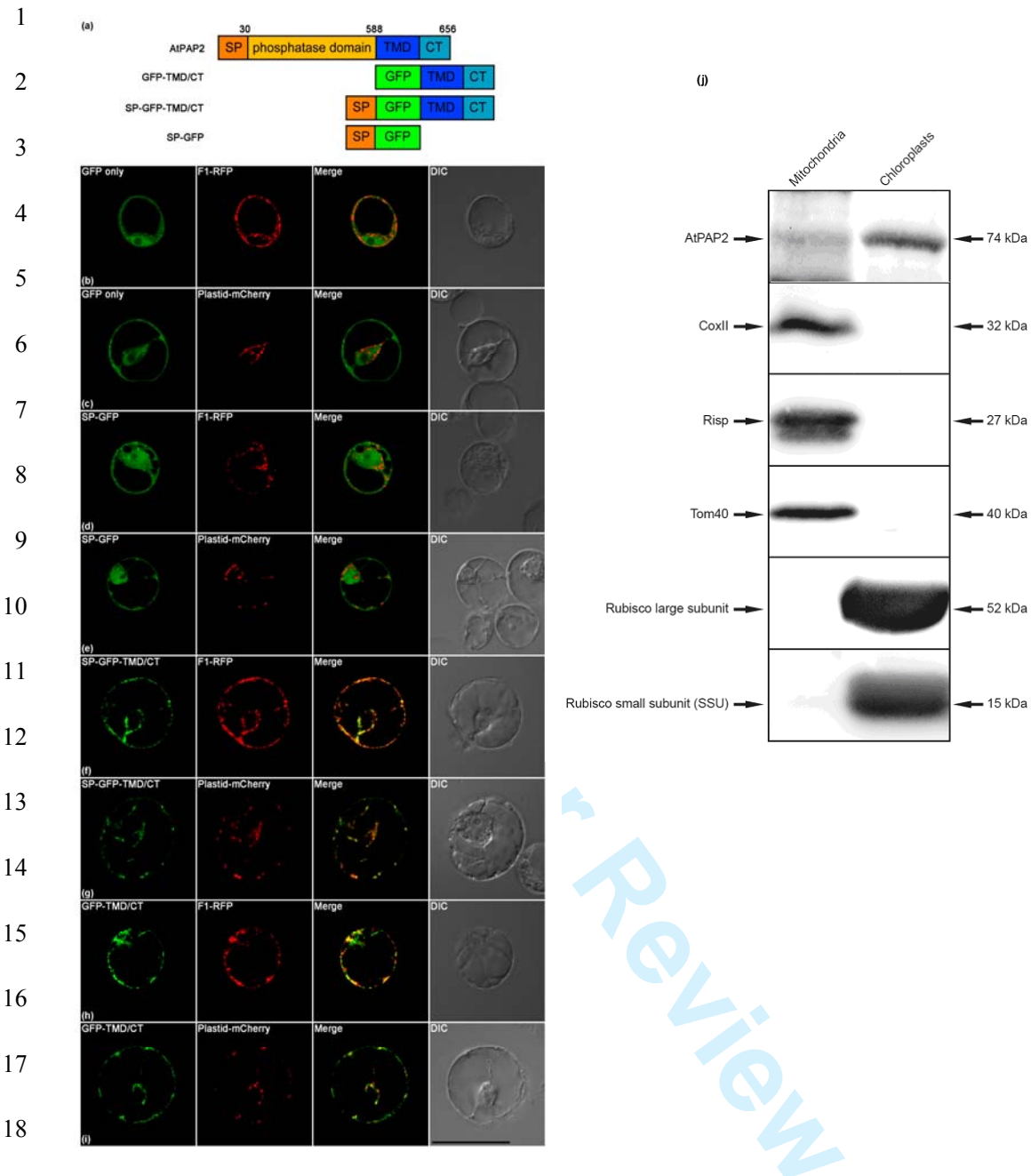| Plant line	WT	T-DNA	OE7	OE21
Sucrose phosphate synthase (μmole sucrose/mg total soluble protein /hour)				
Vmax (Day)	5.44 ± 0.90^a	5.80 ± 0.59^a	7.89 ± 1.08^b	7.97 ± 0.95^b
Vlimit (Day)	3.18 ± 0.32^a	3.47 ± 0.12^a	4.54 ± 0.92^b	3.99 ± 0.68^a
Vmax (Night)	5.91 ± 0.57^a	5.24 ± 0.72^a	7.54 ± 0.97^b	6.82 ± 0.75^a
Vlimit (Night)	3.74 ± 0.31^a	2.83 ± 0.16^b	4.67 ± 0.18^c	4.86 ± 0.54^c
Sucrose synthase (μmole glucose /mg total soluble protein /hour)				
Day	12.46 ± 0.23^a	12.35 ± 1.20^a	12.43 ± 0.22^a	12.76 ± 0.27^a
Night	12.47 ± 0.36^a	12.63 ± 0.44^a	12.54 ± 0.43^a	12.94 ± 0.27^a
Soluble invertase (μmole glucose /mg total soluble protein /hour)				
Day (Acid)	0.71 ± 0.11^a	0.60 ± 0.27^a	0.91 ± 0.45^a	0.90 ± 0.04^a
Night (Acid)	0.70 ± 0.34^a	1.30 ± 0.5^a	0.88 ± 0.21^a	0.69 ± 0.04^a
Day (Alkaline)	8.48 ± 0.49^a	8.06 ± 1.61^a	8.04 ± 1.39^a	8.94 ± 0.84^a
Night (Alkaline)	6.50 ± 0.41^a	5.25 ± 0.63^a	6.80 ± 0.68^a	6.83 ± 0.07^a
Insoluble cell wall invertase (μmole sucrose/mg total soluble protein /hour)				
Day (Acid)	1.11 ± 0.19^a	0.90 ± 0.24^a	1.17 ± 0.31^a	1.20 ± 0.33^a
Night (Acid)	1.08 ± 0.50^a	0.85 ± 0.21^a	1.41 ± 0.21^a	1.11 ± 0.16^a
Day (Alkaline)	6.08 ± 0.14^a	6.35 ± 0.11^a	5.09 ± 0.32^a	5.27 ± 0.10^a
Night (Alkaline)	6.94 ± 0.31^a	7.57 ± 0.43^a	6.17 ± 0.28^a	6.77 ± 0.73^a
Nitrate reductase (μmole nitrite/g fresh weight /hour)				
Middle of the day	0.14 ± 0.00^a	0.15 ± 0.01^a	0.17 ± 0.00^a	0.24 ± 0.02^b
Middle of the night	0.13 ± 0.01^a	0.13 ± 0.00^a	0.15 ± 0.04^{ab}	0.20 ± 0.01^c
Acid phosphatase activity (μmole Pi/mg total soluble protein /hour)				
Middle of the day	8.33 ± 1.38^a	8.05 ± 1.14^a	18.46 ± 1.91^b	16.59 ± 1.04^b
Middle of the night	6.04 ± 0.11^a	6.00 ± 0.81^a	10.71 ± 0.12^b	13.71 ± 0.56^c

47

Fig. 1 Growth phenotypes of AtPAP2 overexpression (OE) and T-DNA inactivation Arabidopsis lines. (a) 4-week-old plants grown under LD conditions. (b) Leaves at day 27 under LD conditions. (c) Dry weight and total leaf area of 40-day-old plants. AtPAP2 OE lines exhibited higher biomass but much lower leaf area at 40 days of age. Leaves were cut (including leaves on inflorescences, if any) and scanned. The leaf area was calculated using Metamorph (www.image1.com). The dry weights of individual plant samples (including leaves) were measured after water evaporation by heat. The experiments were repeated at least 3 times

1

Fig.2 AtPAP2 protein is targeted to both mitochondria and chloroplasts. (a) Targeting of the GFP fusion proteins in Arabidopsis PSB-D protoplasts. Transient expression in Arabidopsis PSB-D protoplasts showed that GFP (GFP only) (b, c) and GFP fused with putative SP region of AtPAP2 (SP-GFP) (d, e) were directed to the cytosol, whereas GFP constructs fused with the TMD/CT region of AtPAP2, including SP-GFP-TMD/CT (f, g) and GFP-TMD/CT (h, i), were co-localized with the mitochondrial (F1-RFP) and chloroplastic (plastid-mCherry) markers. Bar = 50μm. (j). AtPAP2 protein located in both mitochondria and chloroplasts. Western blot of AtPAP2 protein in mitochondria and chloroplasts. (j) Isolated mitochondria and chloroplasts from 10-day-old seedlings were analyzed by western blotting for the presence of

2

1   AtPAP2. Purity of the isolated organelles was determined by blotting with antibodies

2   specific to each organelle. Mitochondria: Cytochrome oxidase subunit II (CoxII), the

3   Rieske iron sulfur cluster binding protein (Risp) and translocase of the outer membrane

4   protein of 40 kDa (Tom40). Chloroplasts: Rubisco large subunit and Rubisco small
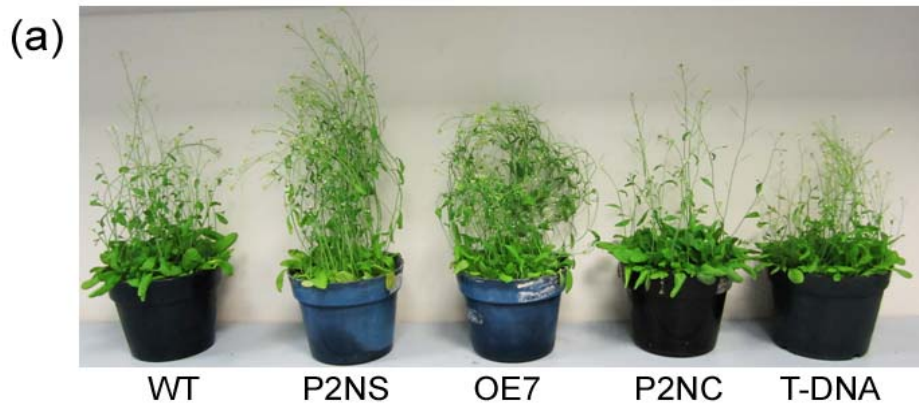
5   subunit (SSU).
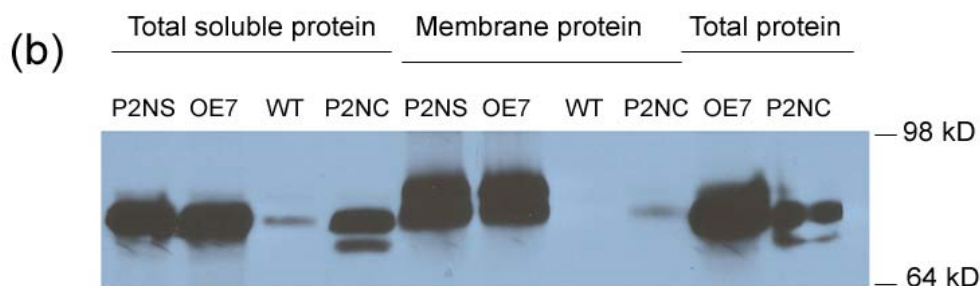
6

7

8

9

10

11

12

13

14

15

16

17

18

19   **Fig. 3** AtPAP2 sublocalization in transgenic plants. (a) Phenotype of 40-day-old plants

20   (n=12) of WT, P2NS (a.a 25-656), OE7 (a.a 1-656), P2NC (a.a 1-588) and *AtPAP2*

21   T-DNA plants. (b) AtPAP2 protein band identification in WT, P2NS, OE7, P2NC and

22   *AtPAP2* T-DNA plants by western blot analysis.
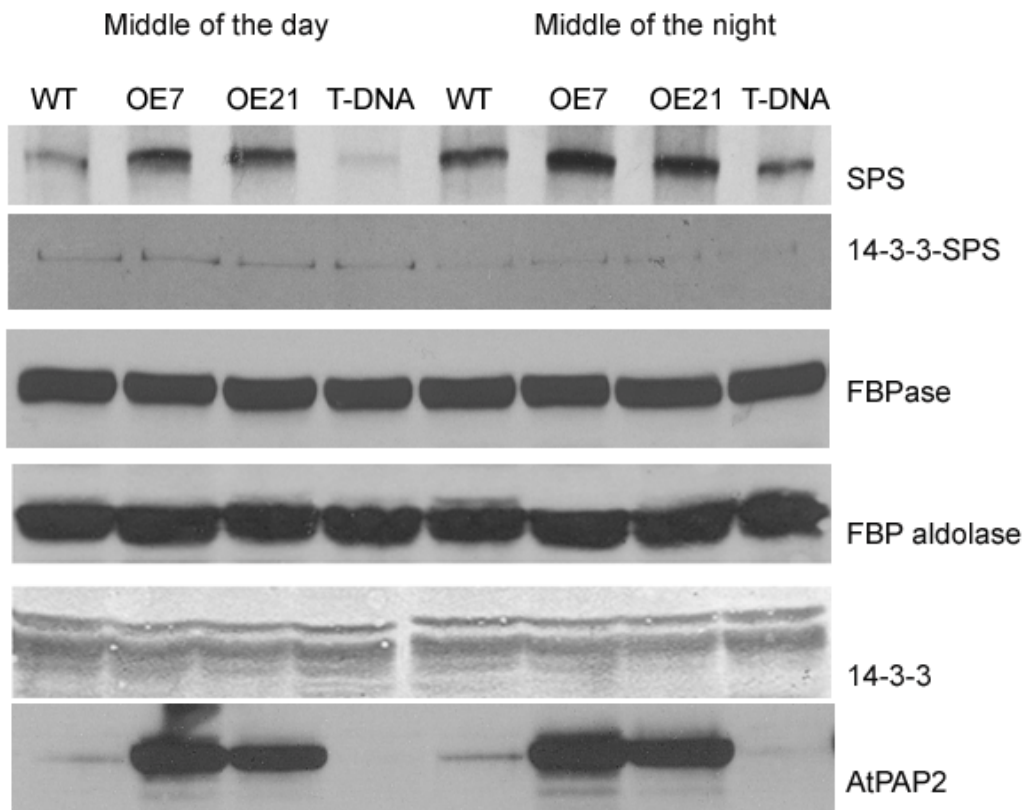
23

24

25

26

27

28

3

Fig. 4 Western blotting of enzymes involved in sucrose biosynthesis. Total soluble protein (30 µg) extracted from the shoots of 20-day-old Arabidopsis was loaded to each lane and was analyzed by western blot using anti-SPS, anti-FBP aldolase and anti-cFBPase antibodies (Agrisera, Sweden). The pulled-down eluates of GST-14-3-3 were diluted 1:1 with 40 µl SDS-sample buffer and half was loaded into each lane.

4

1
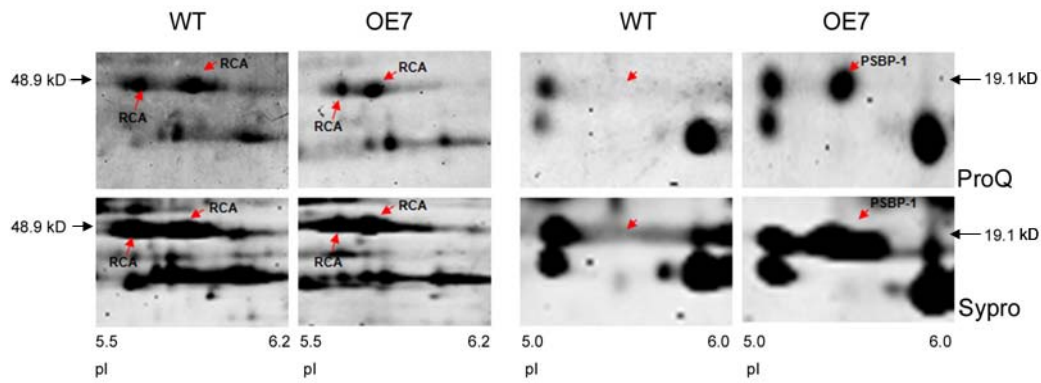
2 **Fig. 5** Analysis of protein from AtPAP2 OE lines. An equal volume of total soluble

3 proteins (300 µg) extracted from 20-day-old Arabidopsis were analyzed by 2-D gel

4 electrophoresis. Gels were stained with Pro-Q Diamond and SYPRO Ruby. The pI

5 range of the gel was 4-7. Targeted spots are identified by the arrows. Mobility shifts of

6 Rubisco activase (RCA) and oxygen-evolving enhancer protein (PSBP-1) are indicated

7 by the arrows. Three biological replicates were used in this study.
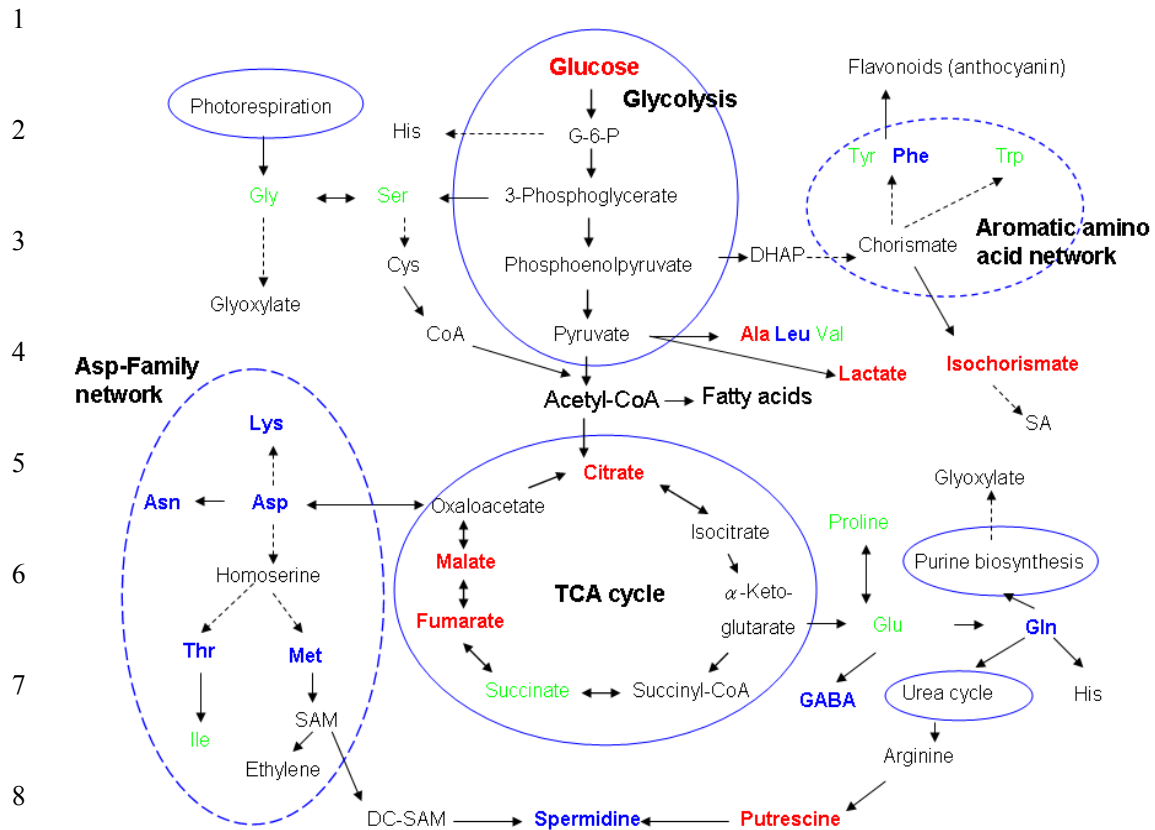
8

9

10

11

12

13

14

15

16

17

18

19

20

21

5

1

Fig. 6 Altered metabolites in the 20-day-old AtPAP2 OE lines. Metabolites in red and blue colors indicate increased or decreased levels in the AtPAP2 OE lines. Metabolites in black were not detected and those in green were unaltered. The dashed blue circles represent the Asp-family and aromatic amino acid network. DHAP, dihydroxyacetone phosphate; GABA, γ-Aminobutyric acid; SA, salicylic acid; DC-SAM, decarboxylated S-adenosyl- methionine.